

EVALUATION OF HIGH PRESSURE / HIGH TEMPERATURE, ECO-FRIENDLY  
IRON SULFIDE SCALE DISSOLVER

A Thesis

by

TAYLOR MAYNE CAMPSEY

Submitted to the Office of Graduate and Professional Studies of  
Texas A&M University  
in partial fulfillment of the requirements for the degree of

MASTER OF SCIENCE

Chair of Committee,	Hisham A. Nasr-El-Din
Committee Members,	Jerome S. Schubert
	Mahmoud El-Halwagi
Head of Department,	Jeffrey Spath

December 2018

Major Subject: Petroleum Engineering

Copyright 2018 Taylor Campsey

## ABSTRACT

A high pressure, high temperature iron sulfide dissolver is not currently on the market. While a dissolver that meets these conditions needs to be developed, the corrosion rate of the dissolver, as well as the hydrogen sulfide evolution need to be considered. Although mineral acids are commonly used for dissolving iron sulfide scales, they can be highly corrosive and are therefore not a good option.

Alternatively, organic acids are more suitable for high temperature conditions but can be significantly more expensive than mineral acids. This study develops an iron sulfide dissolver with an organic and mineral acid blend, corrosion package, hydrogen sulfide scavenging package, iron control agent, and dispersant. Throughout this work, tests were conducted at 320°F and a low pressure range of 400-500 psi and a high pressure range of 1,300-1,400 psi. Reagent grade iron sulfide was used, having an iron to sulfur ratio of 1:1.

The goal of this work is to develop an iron sulfide dissolver package and optimizing each of the chemical additives used. The corrosion rate and the hydrogen sulfide evolution will be considered in the analysis of the dissolver. X-ray diffraction and scanning electron microscope – energy dispersive spectroscopy will be used to identify and confirm the chemical composition of the iron sulfide before the reaction, as well as the after-reaction solids. By utilizing this analysis technique, the changes in the mineral composition can be studied in response to the reaction with different chemicals. Design of experiments will be used to optimize the iron control agent, hydrogen sulfide scavenging aid, and dispersant.

Currently, there is not an iron sulfide dissolving package on the market in the industry that can be used in high pressure and high temperature environments. This package will contribute to the oil and gas industry, allowing for a safe and eco-friendly solution to problematic iron sulfide in wells.

## DEDICATION

This thesis is dedicated to my family. Thank you for supporting me throughout this journey. It would not have been possible without you.

## ACKNOWLEDGEMENTS

I would like to thank my committee chair, Dr. Hisham Nasr-El-Din, and my committee members, Dr. Jerome Schubert and Dr. Mahmoud El-Halwagi, for their guidance and support throughout the course of this research.

Thanks also go to my friends and colleagues and the department faculty and staff for making my time at Texas A&M University a great experience.

Much appreciation goes to Baker Hughes, a GE Company for funding and contributing to this research.

Finally, many thanks to my mother and father for their continuous love and support, as well as my brother, who has made my time in petroleum engineering at Texas A&M University all the more special.

## CONTRIBUTORS AND FUNDING SOURCES

### **Contributors**

This work was supervised by a thesis committee consisting of Professor Hisham Nasr-El-Din and Dr. Jerome Schubert of the Department of Petroleum Engineering and Professor Mahmoud El-Halwagi of the Department of Chemical Engineering.

All work for the thesis was completed by the student, under the advisement of Professor Hisham Nasr-El-Din of the Department of Petroleum Engineering.

### **Funding Sources**

This graduate study was supported by Baker Hughes, a GE Company.

## TABLE OF CONTENTS

	Page
ABSTRACT .....	ii
DEDICATION .....	iv
ACKNOWLEDGEMENTS .....	v
CONTRIBUTORS AND FUNDING SOURCES.....	vi
TABLE OF CONTENTS .....	vii
LIST OF FIGURES.....	ix
LIST OF TABLES .....	xi
CHAPTER I INTRODUCTION AND LITERATURE REVIEW .....	1
1.1    Iron Sulfide Deposition .....	1
1.2    Dissolution of Iron Sulfide Scales.....	3
1.3    Impact of Hydrogen Sulfide Scavengers.....	5
1.4    Research Objectives .....	7
CHAPTER II EXPERIMENTAL STUDIES .....	8
CHAPTER III MATERIALS AND EQUIPMENT .....	14
3.1    Materials.....	14
3.2    Equipment .....	14
CHAPTER IV EFFECT OF INORGANIC AND ORGANIC ACID BLEND ON IRON SULFIDE DISSOLUTION .....	15
4.1    Acid B Experiment.....	15
4.2    Acid A + Acid B Experiment.....	18
4.3    Significance of Organic Acid and Mineral Acid Blend .....	21
CHAPTER V EFFECT OF IRON CONTROL AGENT ON IRON SULFIDE DISSOLUTION .....	22
CHAPTER VI EFFECT OF HYDROGEN SULFIDE SCAVENGERS ON IRON SULFIDE DISSOLUTION .....	30

CHAPTER VII DESIGN OF EXPERIMENTS TO DISSOLVE IRON SULFIDE .....	34
CHAPTER VIII EFFECT OF PRESSURE ON IRON SULFIDE .....	37
CHAPTER VIII CONCLUSIONS AND RECOMMENDATIONS .....	45
8.1    Conclusions .....	45
8.2    Recommendations .....	45
REFERENCES .....	48
APPENDIX A DETAILS OF EXPERIMENTAL METHODS .....	50



## LIST OF FIGURES

	Page
Fig. 1—D8 Advance Eco Bruker X-Ray Diffraction.....	10
Fig. 2—Parr 4521 HT/HP bench top reactor.....	10
Fig. 3— Parr 4521 HT/HP bench top reactor schematic.....	11
Fig. 4—Dräger tube and Accuro manual hand pump used to measure hydrogen sulfide... 12	12
Fig. 5—Mini SEM-EDS.....	13
Fig. 6—Interpreted XRD results for experiment with 35 wt% Acid B.....	16
Fig. 7—Quantitative XRD results for experiment with 35 wt% Acid B. ....	17
Fig. 8—Interpreted XRD results for experiment with 5 wt% Acid A + 5 wt% Acid B. ....	19
Fig. 9—Quantitative XRD results for experiment with 5 wt% Acid A + 5 wt% Acid B. ..	20
Fig. 10—White precipitation noted at high concentrations of iron control agent.....	24
Fig. 11—Interpreted XRD results for high concentrations of iron control agent. ....	25
Fig. 12—Quantitative XRD results for high concentrations of iron control agent. ....	25
Fig. 13—Unreacted iron sulfide at 5x magnification.....	26
Fig. 14—Unreacted iron sulfide at 20x magnification.....	27
Fig. 15—Reacted iron sulfide at 10x magnification. ....	28
Fig. 16—Reacted iron sulfide at 20x magnification. ....	29
Fig. 17—Hydrogen sulfide Scavenger D optimization. ....	31
Fig. 18—XRD analysis for 40 GPT Scavenger D experiment. ....	32
Fig. 19—XRD analysis for 40 GPT Scavenger D experiment. ....	33
Fig. 20—Design of experiments cube.....	35
Fig. 21—Interpreted XRD results for experiment using 400-500 psi.....	38

Fig. 22—Quantitative XRD results for experiment using 400-500 psi.....	39
Fig. 23—Interpreted XRD results for experiment using 1,300-1,400 psi.....	41
Fig. 24—Quantitative XRD results for experiment using 1,300-1,400 psi.....	42
Fig. 25—Parr Reactor Scrubber (Assembled).....	53
Fig. 26—Parr reactor (assembled). ....	54
Fig. 27—Parr reactor (with heater attached). ....	55
Fig. 28—Complete assembled system. ....	56
Fig. 29—Inlet Configuration (1). ....	58
Fig. 30—Inlet Configuration (2). ....	59
Fig. 31—Inlet and outlets of reactor vessel.....	60
Fig. 32—Parr 4523 reactor system.....	61

## LIST OF TABLES

	Page
Table 1—Iron sulfide chemical compositions. ....	2
Table 2—Iron control concentrations on iron sulfide testing. ....	22
Table 3—Hydrogen sulfide scavenger experiments. ....	31
Table 4—Design of experiments concentrations and results. ....	34

## CHAPTER I

### INTRODUCTION AND LITERATURE REVIEW

#### **1.1 Iron Sulfide Deposition**

Iron sulfide scale deposits are becoming increasingly more important in the oil and gas industry. As the scales are formed in downhole or surface conditions, they can plug tubulars, coat safety valves, and cause safety hazards. Upon treatment, hydrogen sulfide, a toxic gas, is released. Iron sulfide deposition in downhole or surface conditions leads to compromised safety and decreased productivity of wells. Iron sulfide is also strongly oil-wet and can change the wettability of the rock, causing emulsions downhole. Many companies are resorting to pulling tubulars rather than attempting to treat or dissolve the iron sulfide scales. Despite the laboratory work and research that has gone into treating iron sulfide over the past several decades, there has not been a safe and economic dissolver developed.

To form iron sulfide scales, a source of iron and sulfur are necessary. These scales are included in the category of exotic scale species due to the sulfur composition. Although ferrous iron can be found in the formation water, the source more commonly is present due to corrosion of the tubulars or equipment. As steel corrodes, the iron is oxidized and is readily available to react with a source of hydrogen sulfide.

Sulfate reducing bacteria (SRB) is a common source of hydrogen sulfide. This bacteria is a type of anaerobe that converts sulfate to sulfide ions. From the sulfide composition, the bacteria can either react with iron, creating iron sulfide, or it can react

with any hydrogen present, forming hydrogen sulfide (Cowan 2005). In Cowan’s study of sulfate reducing bacteria, he also notes how toxic and corrosive the hydrogen sulfide gas is. Not only is it important to avoid sulfide introduction to the system to prevent iron sulfide formation, but also to reduce the hydrogen sulfide evolution. Additionally, hydrogen sulfide can also be introduced to the system from the thermal decomposition of sulfate or during gas lift operations (Nasr-El-Din and Al-Humaidan 2001).

Depending on the amount of iron and sulfur present, different molar ratios of iron sulfide can occur, as seen in **Table 1**. These compositions of iron sulfide include: pyrrhotite ( $\text{Fe}_7\text{S}_8$ ), troilite ( $\text{FeS}$ ), marcasite ( $\text{FeS}_2$ ), pyrite ( $\text{FeS}_2$ ), greigite ( $\text{Fe}_3\text{S}_4$ ), and mackinawite ( $\text{Fe}_9\text{S}_8$ ) (Taylor et al. 1999). At shallower depths, the ratio of iron to sulfur decreases and becomes less soluble in acid due to more exposure to hydrogen sulfide; alternatively, the deeper locations in the well have had less exposure to hydrogen sulfide, and have molar ratios that are closer to unity (Nasr-El-Din and Al-Humaidan 2001). As the composition of iron sulfide changes, and the iron sulfide has more exposure to a sulfide source, the sulfur surrounds the iron. As the sulfur ions become more prevalent around the iron ions, the acid reaction is prevented, making iron sulfide unable to be dissolved.

Mineral Name	Chemical Composition
Mackinawite	$\text{Fe}_9\text{S}_8$
Troilite	$\text{FeS}$
Greigite	$\text{Fe}_3\text{S}_4$
Pyrrhotite	$\text{Fe}_7\text{S}_8$
Pyrite	$\text{FeS}_2$
Marcasite	$\text{FeS}_2$

**Table 1—Iron sulfide chemical compositions.**

Each of the iron sulfide phases exists at certain conditions and can change with temperature, pressure, or additional hydrogen sulfide exposure. Troilite is a very common, stable form of iron sulfide with a molar ratio between iron and sulfur of unity. The cubic FeS state is a transition between mackinawite and troilite, but due to instability, it is very uncommon and rarely seen. When the troilite state is reached, the next phase is pyrrhotite, followed by pyrite or marcasite given the conditions.

## 1.2 Dissolution of Iron Sulfide Scales

Scale dissolution tests consist of allowing a reaction to occur between a scale and a treatment system, or dissolver, at a desired temperature and pressure to test the effectiveness of the scale dissolver. Ford et al. (1992) showed the reaction between iron sulfide and hydrochloric acid (HCl), which produces hydrogen sulfide and ferrous chloride (**Eq. 1**).



In **Eq. 2** and **Eq. 3**, troilite and pyrrhotite, respectively, iron and sulfur have a molar ratio approaching unity; when the ratio is closer to unity, the scale is more reactive with acid treatment. In this case, when iron sulfide has a 1:1 molar ratio, mechanical jetting can be combined with chemical treatments, which increases the effectiveness of the treatment. Alternatively, in Eq. 4, the molar ratio of iron and sulfur is 1:2. These types of

iron sulfide, such as marcasite or pyrite, are not reactive with acid and cannot be dissolved through chemical means. Due to the sulfur surrounding the iron ions, the acid is unable to react. Therefore, it is more common to pull and replace the tubulars, rather than trying to treat the iron sulfide scales.

The reaction kinetics of iron sulfide are also an important factor when studying iron sulfide solubility. Lawson et al. (1980) investigated the reaction rate of iron sulfide with hydrogen and identified the forward and reverse reactions (**Eq. 4**).

$$\text{Rate} = k_f[\text{H}^+] - k_r[\text{Fe}^{2+}]^{0.5}(\text{P}_{\text{H}_2\text{S}})^{0.5} \quad (4)$$

Where  $k_f$  is the forward reaction, controlled by the hydrogen atoms, and  $k_r$  is the reverse action, controlled by ferrous iron and the partial pressure of hydrogen sulfide. This reaction is important to note because as hydrogen sulfide stays in solution, the reaction does not progress. The dissolution treatment of iron sulfide needs to include a hydrogen sulfide scavenger to remove hydrogen sulfide in the reaction, which will maintain the forward reaction. A hydrogen source is needed to act as a dissolver for iron sulfide. This also supports that as pressure increases, the solubility of iron sulfide decreases.

Nasr-El-Din and Al-Humaidan (2000) investigated the reaction between iron sulfide and hydrochloric acid, in addition to different additives. They found that all reagent grade iron sulfide was dissolved with 20 wt% HCl. However, as the temperature downhole increases, the HCl becomes increasingly more corrosive. Significantly higher loading of corrosion inhibitors and intensifiers need to be used to protect downhole equipment.

However, these corrosion packages oftentimes work against the HCl and iron sulfide reaction. When looking at additives, not only corrosion inhibitors, but also hydrogen sulfide scavengers, iron control agents, and clay stabilizers often form a coating over the iron sulfide particles that prevent reactions with the acid when used at high concentrations. Therefore, it becomes much less efficient to use high concentrations of HCl, such as 20 wt%. Due to the corrosive nature of hydrochloric acid, specifically at high temperatures, it is widely agreed upon that a safe and economic solution to address dissolving iron sulfide needs to be found.

Using organic acid alone as a dissolver has not been successful when treating iron sulfide, regardless of pH and concentration. Elkatatny (2017) developed a formulation combining organic acid and mineral acid combined, and it was tested up to 125°C with success. This treatment was reported to dissolve 78% of iron sulfide after 24 hours. By introducing a mineral acid, such as HCl, the cost of the treatment is decreased due to the expensive nature of organic acid. Rather than using mineral acid alone, the combination of mineral and organic acid offers a less corrosive iron sulfide dissolving solution.

### **1.3 Impact of Hydrogen Sulfide Scavengers**

Hydrogen sulfide is an undesirable gas that is released when many dissolvers react with iron sulfide, as well as in many different hydrocarbon fields and streams. The corrosive nature and hazards related to hydrogen sulfide release can damage equipment, in addition to being toxic and harming personnel. When dissolving iron sulfide or dealing with sour



wells, hydrogen sulfide scavengers need to be considered and implemented. Two of the most common scavengers in hydrocarbon producing wells include triazine and glyoxyl.

Although triazine is one of the most widely used hydrogen sulfide scavengers, it suffers major limitations. MEA triazine, or 1,3,5-tris(2-hydroxyethyl)hexahydro-s-triazine, and MMA triazine, or 1,3,5-trimethyl-hexahydro-s-triazine are the two most commonly used triazines. Chakraborty et al. (2017) states that hydrolysis unfavorably affects the reaction of triazine, and more so at a  $\text{pH} < 10$ . Additionally, hydrolysis affects MEA triazine 20 times more than MMA triazine (Buhaug et al., 2002). Triazine has difficulties scavenging effectively at low pH conditions and can precipitate insoluble scale deposits. Because most iron sulfide dissolvers are acidic, triazine has not worked well in this application.

Glyoxyl is a more widely used alternative scavenger to triazine. However, one of the major drawbacks is glyoxyl is the scavenger is highly corrosive; therefore, it cannot be used in gas tower applications (Keenan et al., 2015). Bedford et al. (1992) has proven that one of the reaction products between glyoxyl and hydrogen sulfide is the crystalline adduct formed with three glyoxyl and two hydrogen sulfide molecules:  $(\text{C}_2\text{H}_2\text{O}_2)_3(\text{H}_2\text{S})_2$ .

Frenier and Hill (1999) present an invention that combines aliphatic aldehydes and aromatic aldehydes in acidizing treatments. The aliphatic aldehyde mentioned, glyoxyl, should have 1-6 carbon atoms. The aromatic aldehyde, preferably cinnamaldehyde, should have 7-10 carbon atoms. The authors of this patent elaborate on the success of this treatment with non-oxidizing mineral acids and with non-oxidizing organic acids. The combination of the aromatic aldehyde and aliphatic aldehyde scavenge hydrogen sulfide,

while reducing the corrosion rate of the treatment by forming a coating over metals (Frenier and Hill 1999). The authors' recommended weight ratio between glyoxylic acid and cinnamaldehyde is 10:1. At this ratio, Frenier and Hill (1999) did not find that the solution coated the iron sulfide or interfered with the dissolution reaction.

#### **1.4 Research Objectives**

The aim of this research is to develop a high efficiency iron sulfide scale dissolver, while considering the following:

1. Minimal hydrogen sulfide evolution upon reaction with iron sulfide
2. Acceptable corrosion and pitting rating
3. The effect of scavenger aids, iron control agents, and dispersants on iron sulfide dissolution and suspension
4. The effects of iron control agents on total dissolution, considering re-precipitation.

## CHAPTER II

### EXPERIMENTAL STUDIES

To maximize iron sulfide dissolution and minimize hydrogen sulfide evolution, a formula consisting of an acid dissolver, corrosion package, hydrogen sulfide scavenger, dispersing agent, and iron control agent was formulated. The corrosion properties of the acid were considered when developing the dissolver.

A mineral acid (Acid A) and an organic acid (Acid B) were tested to see the dissolution efficiency of iron sulfide. Three different corrosion packages were tested by Baker Hughes, which included a corrosion inhibitor and intensifier. To minimize the hydrogen sulfide evolution, two H<sub>2</sub>S scavengers were tested. A surfactant was used to disperse the iron sulfide during and after the reaction. Chelating agents were tested as iron control to increase the efficiency of iron sulfide dissolution and minimize re-precipitation.

Reagent grade iron sulfide fused rods, with an iron to sulfur molar ratio of 1:1, were used for the experimental research. The rods were ground using an agate mortar and pestle to prevent contamination. Particles of 106-150 microns were sieved and used for the tests to maintain a consistent surface area. X-ray diffraction was used to confirm the iron sulfide

composition before the reaction (

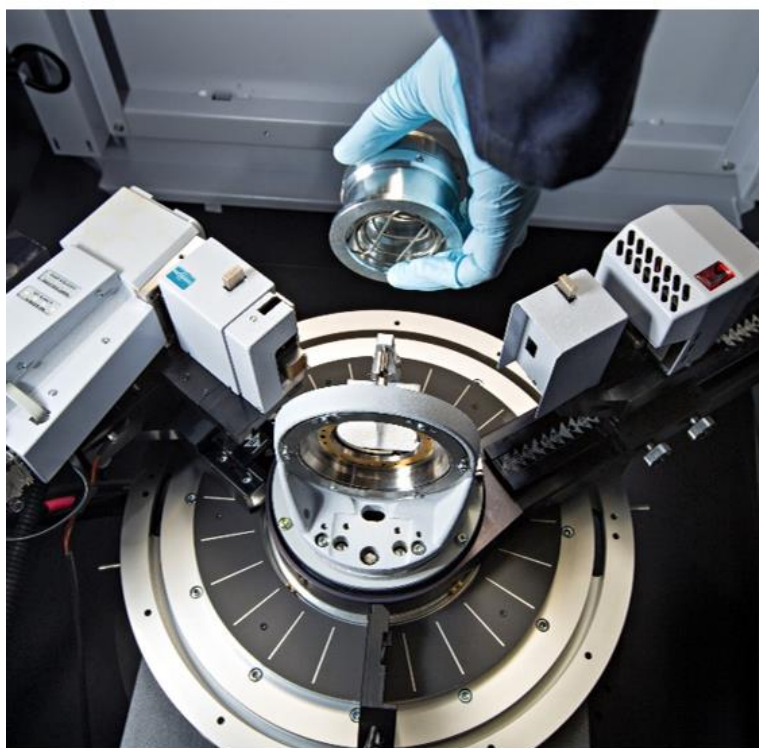


**Fig. 1).**

To develop a dissolver for high temperature conditions, the reactions were tested at 320°F. Two different pressure ranges were used to determine the effect of pressure on the scale dissolution, 300-400 psi and 1,300-1,400 psi. The acid to iron sulfide ratio used was 20:1. The acid and iron sulfide were mixed and placed inside a Parr 4520 Bench top reactor (**Fig. 2, Fig. 3**).

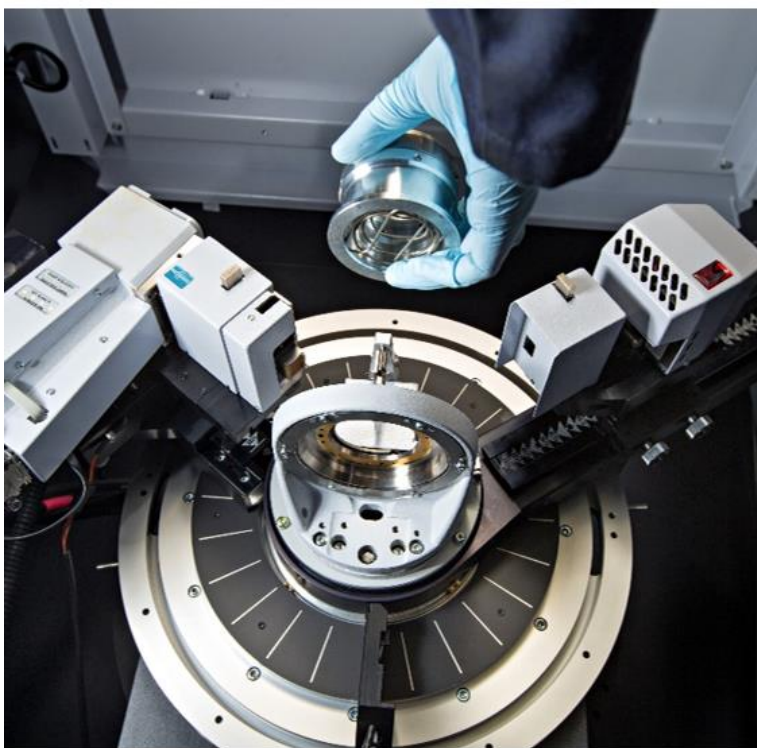


**Fig. 1—D8 Advance Eco Bruker X-Ray Diffraction.**



**Fig. 2—Parr 4521 HT/HP bench top reactor.**

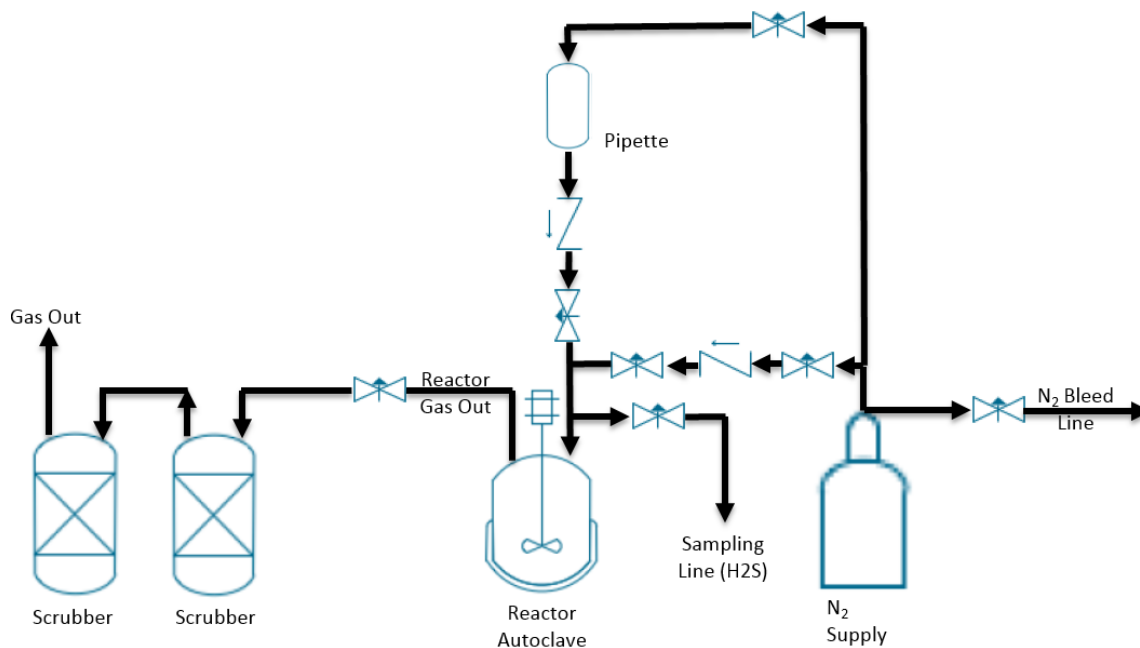


**Fig. 3— Parr 4521 HT/HP bench top reactor schematic.**

The reactor was pressurized and purged using nitrogen. The purging of the system was to ensure that the oxygen was removed to prevent the formation of iron oxide. The system was pressurized to 300-400 psi or 1,300-1,400 psi, dependent on the experimental conditions, and heated to 320°F using a heating jacket. The reaction occurred for four hours.

At the end of the four hour reaction, the heating jacket was removed and the system was allowed to cool without aid to prevent any sudden temperature changes. At 175°F and approximately 1,000 psi, a Dräger tube and Accuro manual hand pump (**Fig. 4**) were used to test the hydrogen sulfide concentration directly from the reactor vessel. The gas was sampled using a hydrogen sulfide compatible sampling bag. After sampling, the reactor

was allowed to cool to room temperature before being depressurized through two sodium hydroxide scrubbers to neutralize the hydrogen sulfide gases (**Eq. 5**). The reactor was purged with nitrogen after the reaction to ensure the free hydrogen sulfide was removed.



**Fig. 4—Dräger tube and Accuro manual hand pump used to measure hydrogen sulfide.**

The after reaction solid and acid solution was filtered using a 1-5 micron filter. The spent acid was collected, and the solids were rinsed with deionized water and acetone to remove the acid from the particles. The solids were dried at 140°F for 12 hours before being

weighed. The dissolution was calculated based on the weight of iron sulfide before and after the reaction (**Eq. 6**).

$$\text{Dissolution, \%} = \frac{m_{\text{initial}} - m_{\text{final}}}{m_{\text{initial}}} \times 100 \quad (6)$$

X-ray diffraction was used to analyze the after-reaction solids to determine the mineralogical composition. Scanning electron microscope—energy dispersive spectroscopy (SEM-EDS) was used to confirm the elemental composition of the solids (**Fig. 5**).



**Fig. 5—Mini SEM-EDS.**



## CHAPTER III

### MATERIALS AND EQUIPMENT

#### **3.1 Materials**

All chemicals used for the dissolver were supplied by Baker Hughes, a GE Company for this study, including: an organic acid, a mineral acid, iron control agents, corrosion inhibitors, corrosion inhibitor intensifiers, hydrogen sulfide scavengers, scavenger aids, and dispersants. The acid formula was prepared by dilution with de-ionized water having a resistivity of 18.2  $\Omega$ M at room temperature, or 77°F. Reagent grade iron sulfide rods were obtained from Sigma Aldrich and had an iron to sulfur ratio of 1:1. The rods were ground using an agate mortar and pestle to prevent contamination. Acetone and de-ionized water were used to remove the acid from the solid samples after testing.

#### **3.2 Equipment**

- 1) A drying oven to dry the iron sulfide after the reaction
- 2) Agate mortal and pestle to grind the iron sulfide
- 3) D8 Advance Eco Bruker X-Ray Diffraction to test the mineralogical composition of the solid samples
- 4) SEM-EDS to test the chemical composition of the solid samples
- 5) Drager tube and Accuro manual hand pump to measure hydrogen sulfide
- 6) Parr 4521 HT/HP bench top reactor

## CHAPTER IV

### EFFECT OF INORGANIC AND ORGANIC ACID BLEND ON IRON SULFIDE DISSOLUTION

#### **4.1 Acid B Experiment**

A maximum concentration of Acid B, the organic acid, of 35 wt% was given by the providing company. To have a base comparison, a test was conducted with 35 wt% Acid B + 30 GPT Scavenger D + 12 GPT CI. The conditions of this experiment were 320°F and 1,300-1,400 psi. The resulting dissolution after 4 hours of testing was 55 wt% of the solid iron sulfide sample. X-ray diffraction was performed on the sample to analyze the change in chemical composition.

The **Fig. 6** shows the raw, overlaid with interpreted, results for the test with 35 wt% Acid B. It should be noted that the sample was noisy and interpretation was difficult. Picotpaulite, a common mineral found when mining sulfide ores, consists of tellurium, iron, and sulfur. Yavapaiite is a potassium, iron, and sulfate based mineral, which accounted for the majority of the interpretation. Pyrrhotite, a form of iron sulfide with the iron to sulfur ratio of approximately 1:1, consisted of 18% of the sample. The last element that was interpreted was quartz, an unexpected mineral. It is assumed that this is due to contamination of the sample during grinding with the agate mortar and pestle.

It should also be noted that a large peak at approximately 18 2Theta was unable to be identified.

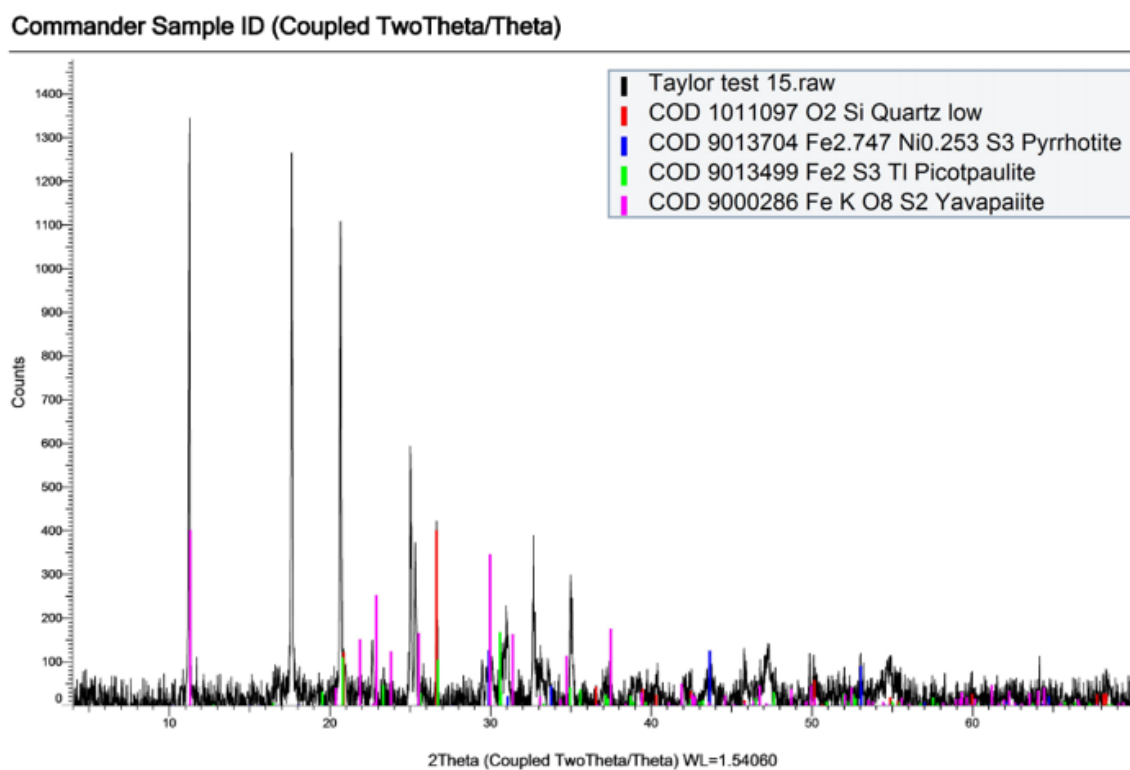


**Fig. 6—Interpreted XRD results for experiment with 35 wt% Acid B.**

The quantitative results of the 35 wt% Acid B experiment can be seen in **Fig. 7**. The after reaction solid sample consisted of 52% yavapaiite, 18% pyrrhotite, 23% quartz, and 7% picotpaulite.

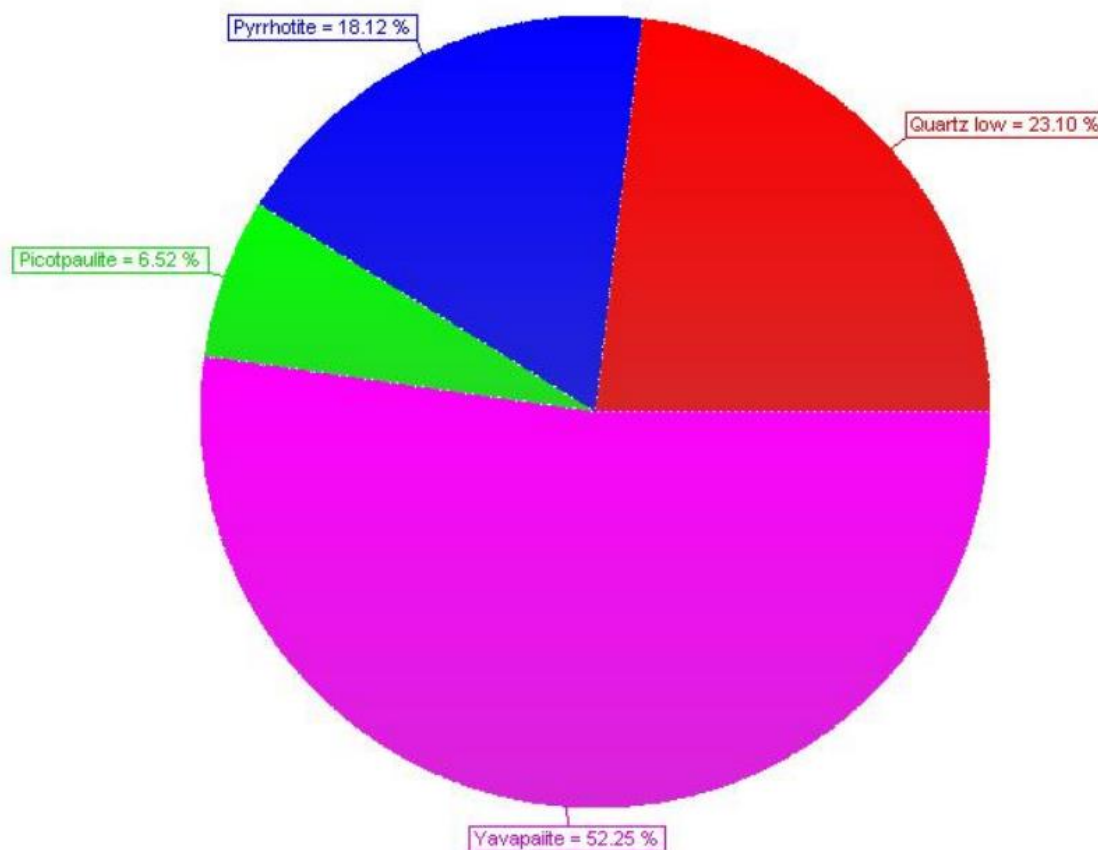


**Fig. 7—Quantitative XRD results for experiment with 35 wt% Acid B.**

## 4.2 Acid A + Acid B Experiment

To decrease the amount of organic acid being used, a mineral acid was introduced. Because of the highly corrosive nature, especially at high temperature, only 5 wt% of Acid A was used. A test was conducted with 5 wt% Acid A + 5 wt% Acid B + 30 GPT Scavenger D + 12 GPT CI. The conditions of this experiment were 320°F and 1,300-1,400 psi. The resulting dissolution after 4 hours of testing was 52 wt% of the solid iron sulfide sample. X-ray diffraction was performed on the sample to analyze the change in chemical composition.

In **Fig. 8**, the raw XRD results, overlaid with the interpretation can be seen. Although the sample is noisy, six major peaks can be identified. The pyrrhotite mineral, which has a nearly 1:1 ratio between iron to sulfur, perfectly matches each of the major six peaks.

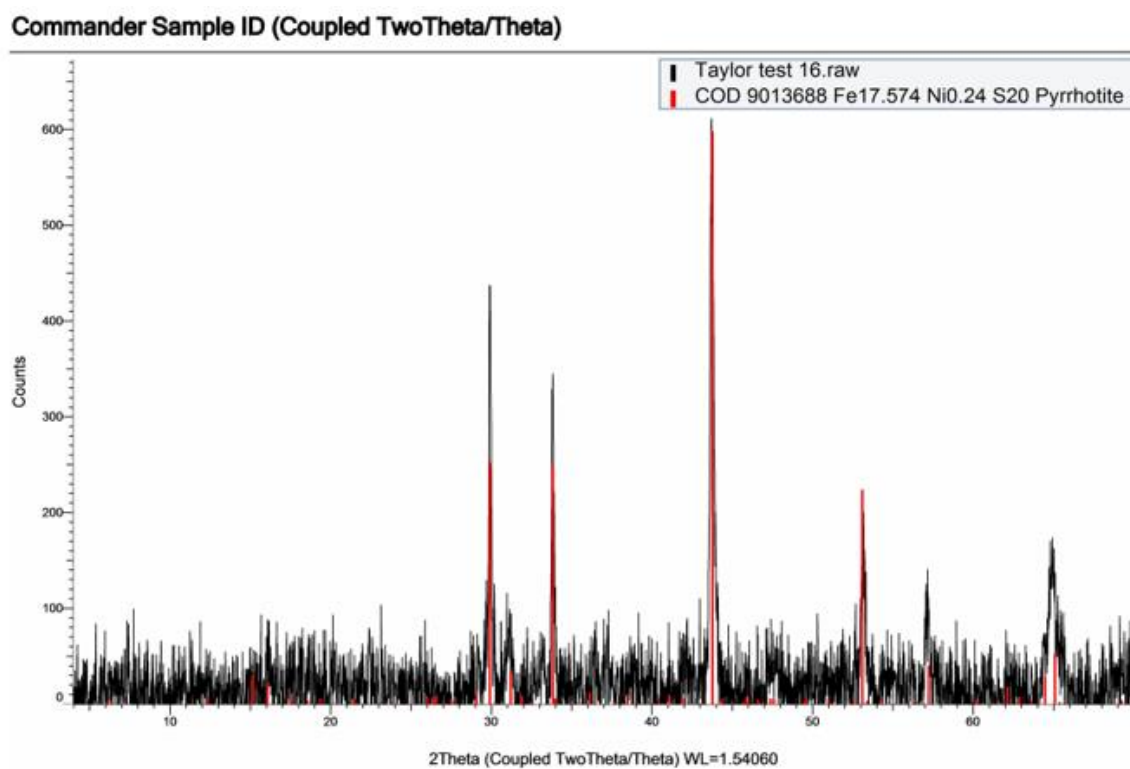


**Fig. 8—Interpreted XRD results for experiment with 5 wt% Acid A + 5 wt% Acid B.**

The quantitative results of the 5 wt% Acid A + 5 wt% Acid B experiment can be seen in **Fig. 9**. The after reaction solid sample consisted of 100% pyrrhotite (iron sulfide).

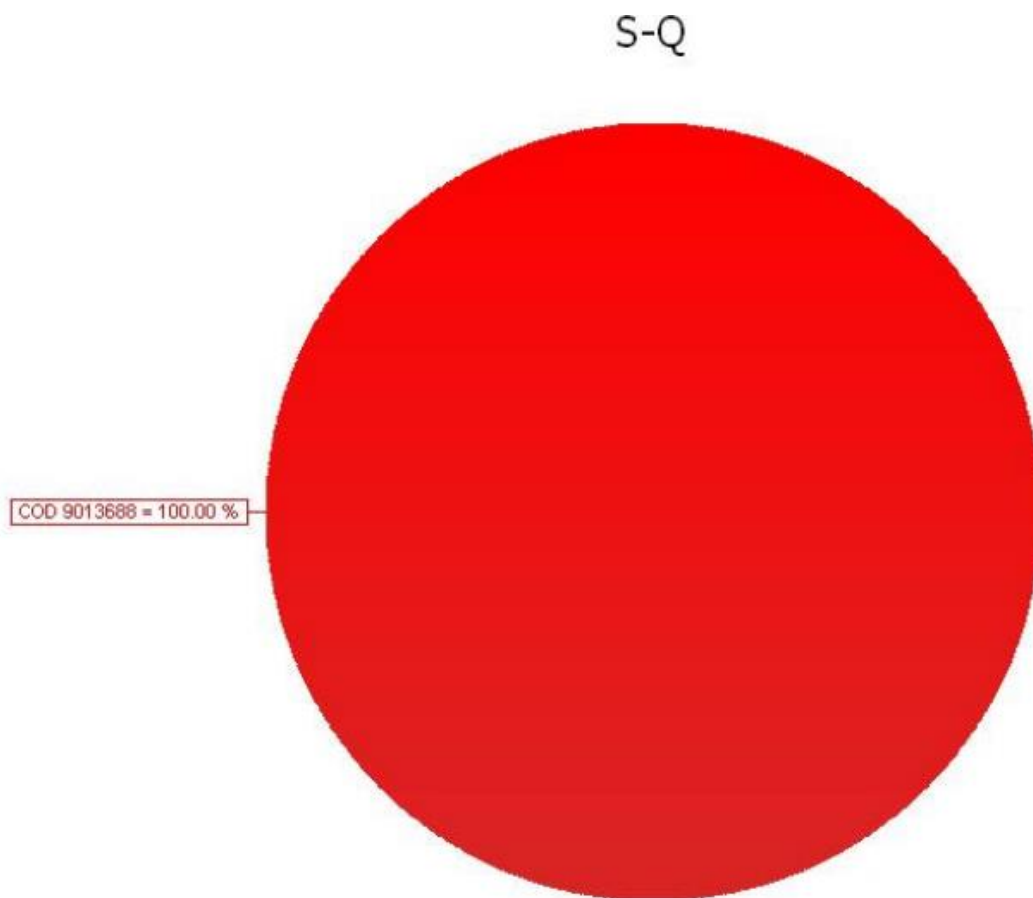


**Fig. 9—Quantitative XRD results for experiment with 5 wt% Acid A + 5 wt% Acid B.**

### **4.3 Significance of Organic Acid and Mineral Acid Blend**

The results from section 4.1 and 4.2 prove to be highly significant for several reasons. First, the addition of the 5 wt% Acid A, or mineral acid, allows for a decrease of Acid B, or the organic acid, from 35 wt% to 5 wt%. This decrease is saves significant costs due to the expensive nature of organic acids.

Additionally, the after reaction sample is interpreted as 100% iron sulfide, rather than four different, and difficult to interpret, minerals. Iron sulfide can be dissolved with acid, suggesting that a second acid treatment or longer contact period may increase dissolution.

At 35 wt% Acid B, the dissolution of the iron sulfide was 55 wt%. When using only 5 wt% Acid A + 5 wt% Acid B, the dissolution was a comparable 52 wt%. This decrease in Acid B is cost effective and decreases the total acid content of the solution.



## CHAPTER V

### EFFECT OF IRON CONTROL AGENT ON IRON SULFIDE DISSOLUTION

To determine the most effective method for iron control, a chelant was tested at varying concentrations shown in **Table 2**. The iron control agent was tested for the effect on the iron sulfide dissolution and hydrogen sulfide evolution. The testing conditions were 1,300-1,400 psi and 320°F.

Test	Concentration	Dissolution, wt%	Hydrogen Sulfide, ppm	Remainer of System
1	0 GPT	52	600	5 wt% Acid A + 5 wt% Acid B + 30 GPT Scavenger D + 12 GPT CI
2	1.5 GPT	74	700	
3	1:1 molar ratio	-50	0	

**Table 2—Iron control concentrations on iron sulfide testing.**

Initial screening was done to see the effect of the iron control agent. In later experiments, the iron control agent was a part of design of experiments to determine the most efficient concentration.

All tests had acid systems had the same concentrations of Acid A and Acid B, utilizing the positive effects from combining a mineral and organic acid. Additionally, the hydrogen sulfide scavenger was optimized, and the most efficient concentration of 30 GPT was used. In consistency with all tests prior to design of experiments, 12 GPT of CI was used for protection of the experimental equipment.

Without the iron control agent, 52% of iron sulfide was dissolved, while releasing 600 ppm of hydrogen sulfide. By adding 1.5 GPT of the iron control agent, per

recommendation of the providing company, 74% of iron sulfide was dissolved, while releasing 700 ppm of hydrogen sulfide. The addition of the 1.5 GPT of the iron control agent increased dissolution by 22%, but only increased the hydrogen sulfide evolution by 100 ppm. The chelant was able to grab the iron to keep it from reacting back with the hydrogen sulfide and reversing the reaction, shown in **Eq. 6**.



To test the chelant at a 1:1 molar ratio between chelant and iron, an experiment was conducted with the mentioned concentrations. It was expected that each mole of chelant would chelate one mole of iron, but due to the iron sulfide not dissolving entirely, there was excess chelant. There was a 50% increase in the weight of the after reaction solids, and white precipitation was noted, shown in **Fig. 10**.



**Fig. 10**—White precipitation noted at high concentrations of iron control agent.

XRD was conducted to determine the composition of the after reaction solids. The XRD results can be seen in **Fig. 11** and **Fig. 12**.

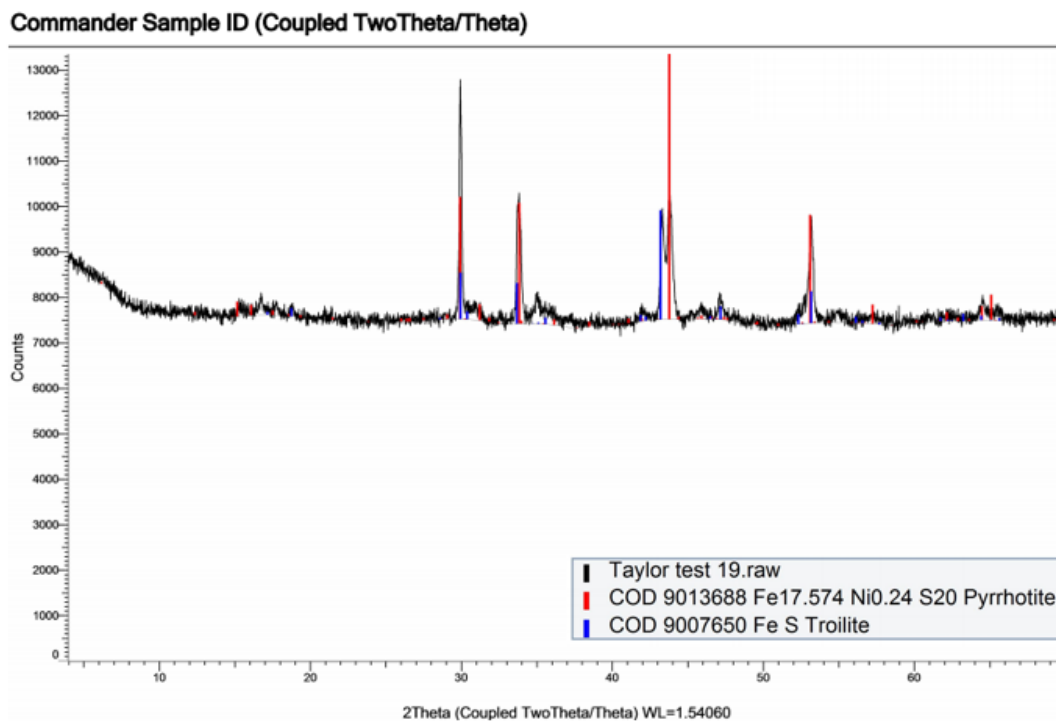


Fig. 11—Interpreted XRD results for high concentrations of iron control agent.

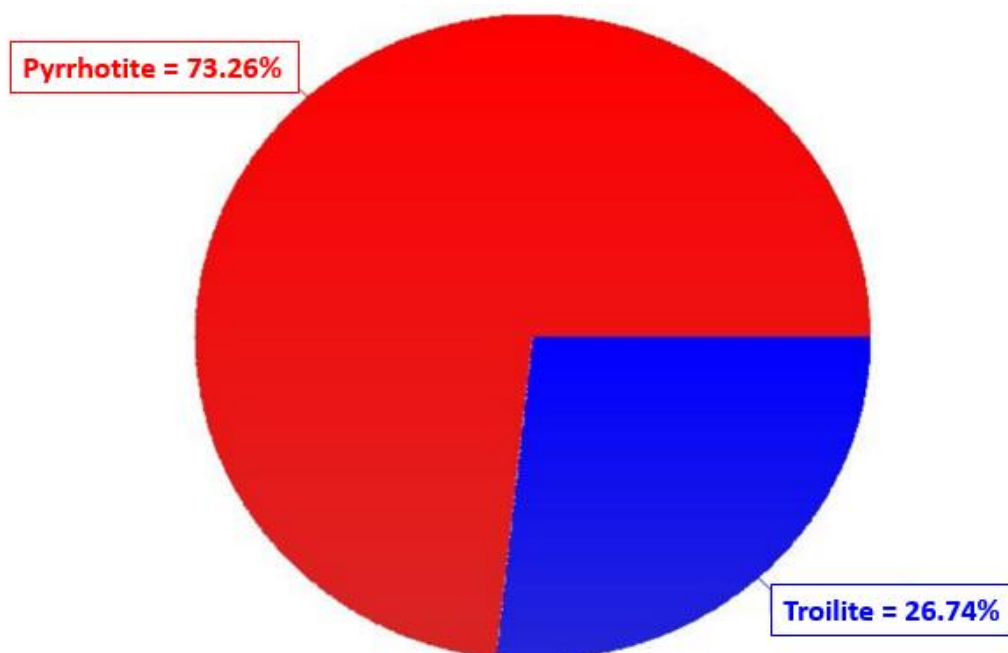
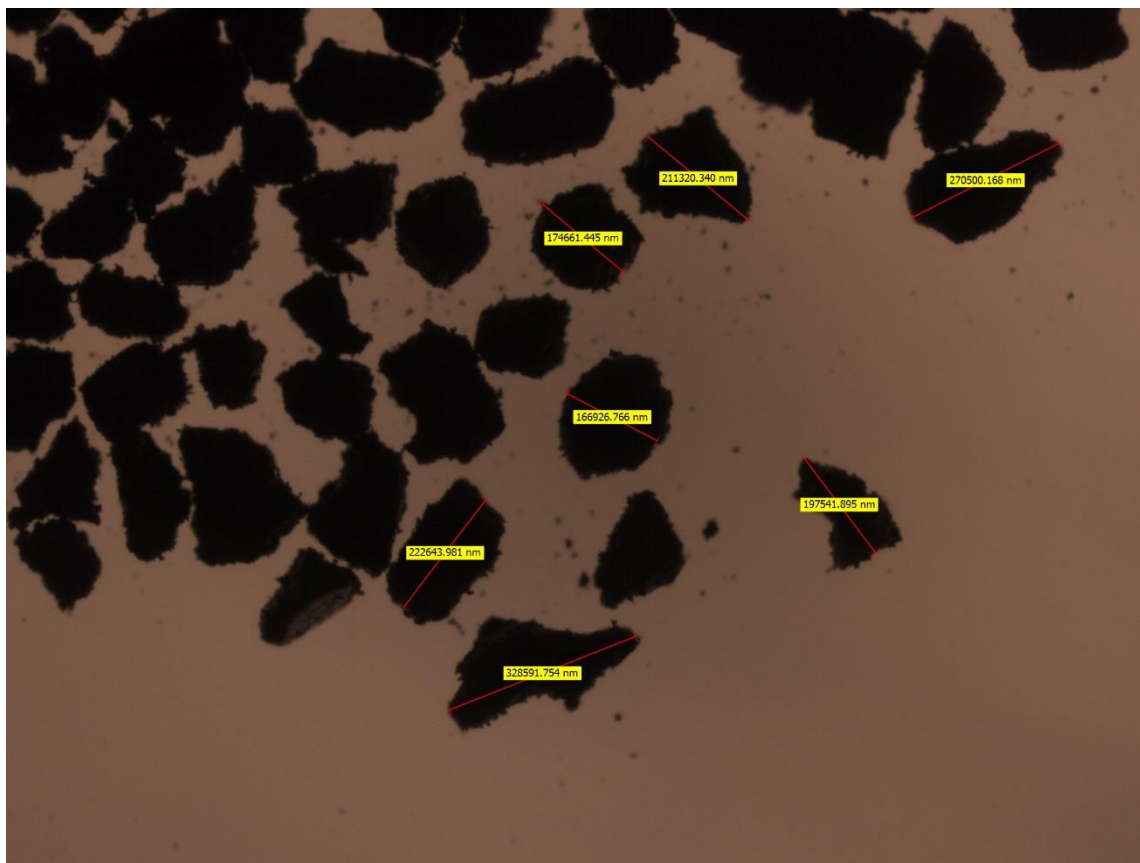


Fig. 12—Quantitative XRD results for high concentrations of iron control agent.

The XRD test had five distinct peaks, and from the interpretation of the results, they were identified as pyrrhotite and troilite. Both identified compositions are forms of iron sulfide that have iron to sulfur ratios of approximately unity. Based on these results, the XRD was unable to pick up the precipitation, suggesting the white material did not have a crystalline structure.

For further analysis, the optical microscope was used to better visualize the precipitation from the high concentration of iron control agent test. Unreacted iron sulfide can be seen in **Fig. 13** and **Fig. 14**.



**Fig. 13—Unreacted iron sulfide at 5x magnification.**

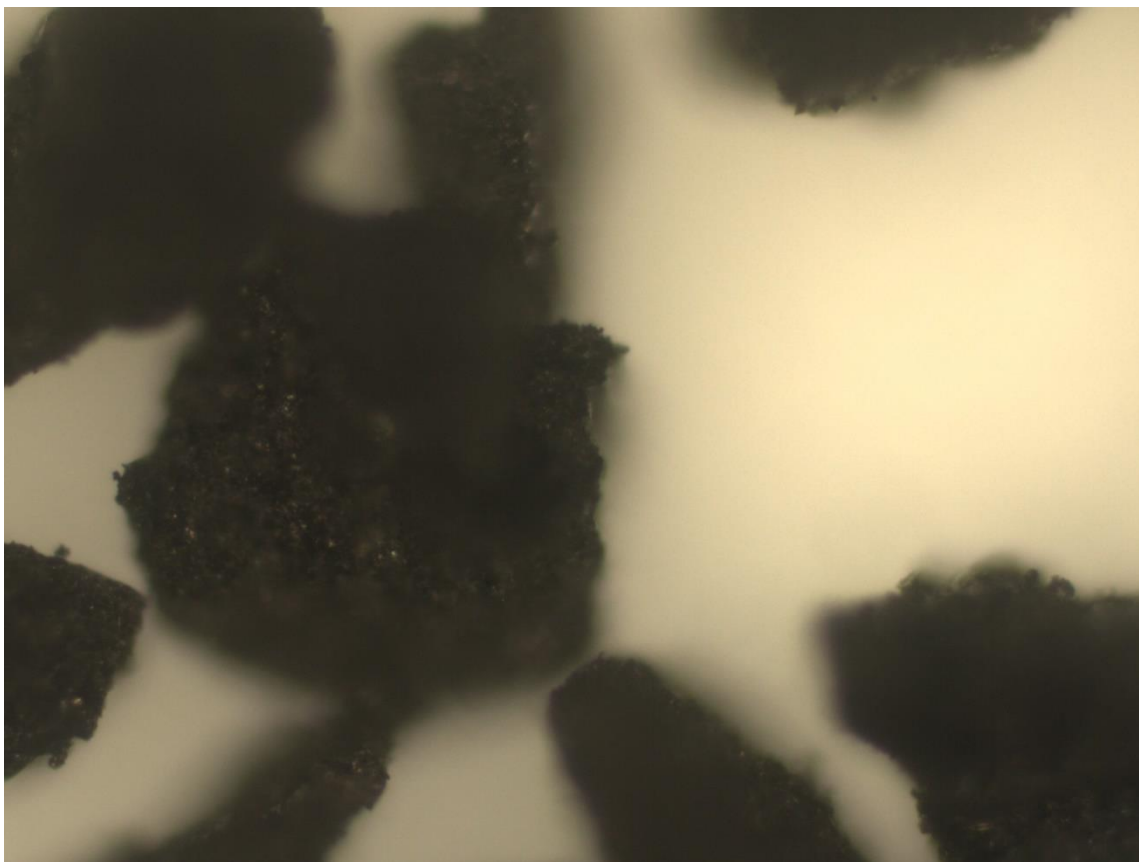


**Fig. 14—Unreacted iron sulfide at 20x magnification.**

The unreacted iron sulfide, or the solids that did not have any contact with acid, appear to be black solid particles with some sharp edges. There is not any apparent discoloration in the sample.

In comparison, the iron sulfide from Test 3 was examined under the optical microscope at 10x magnification, shown in **Fig. 15**. Some reddish-orange discoloration was noted at 10x magnification, suggesting oxidation.

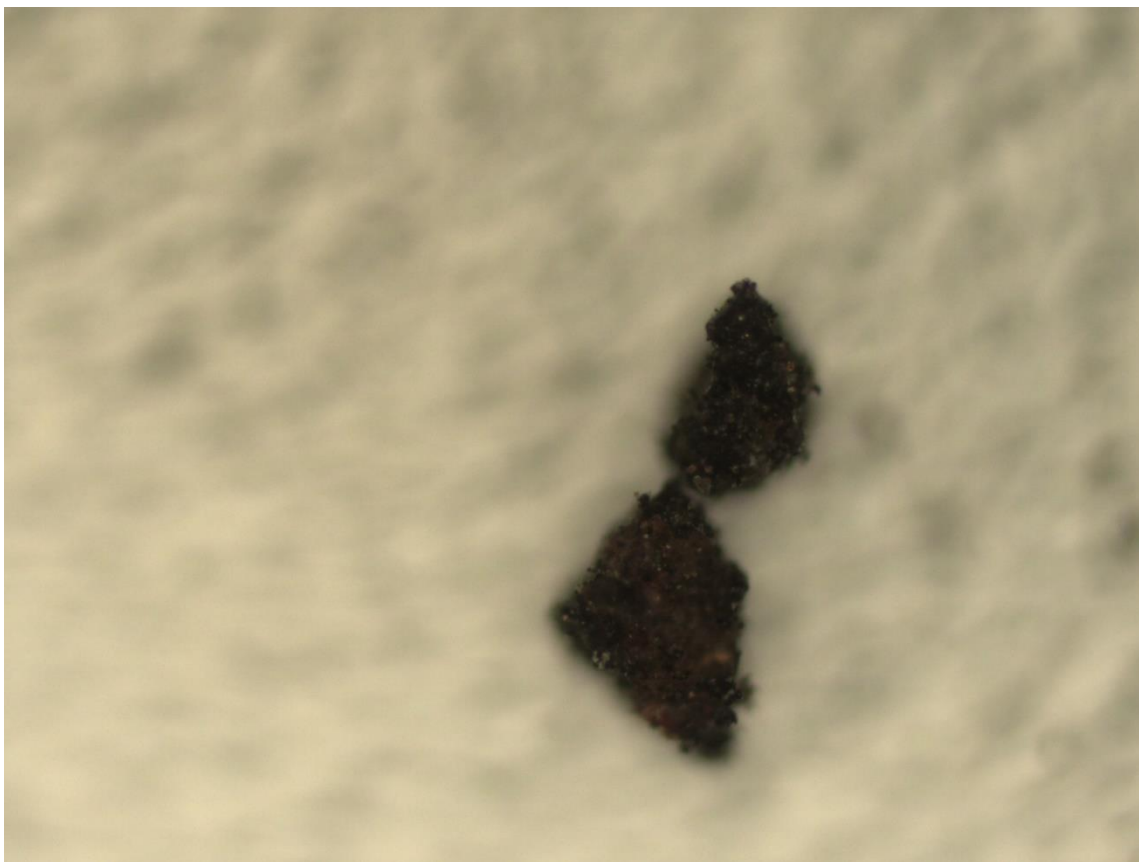


**Fig. 15—Reacted iron sulfide at 10x magnification.**

In **Fig. 16**, white precipitation can be seen on the iron sulfide particles when examined at 20x magnification. Additionally, the particles do not appear to be as solid, but more so no conglomeration is seen.

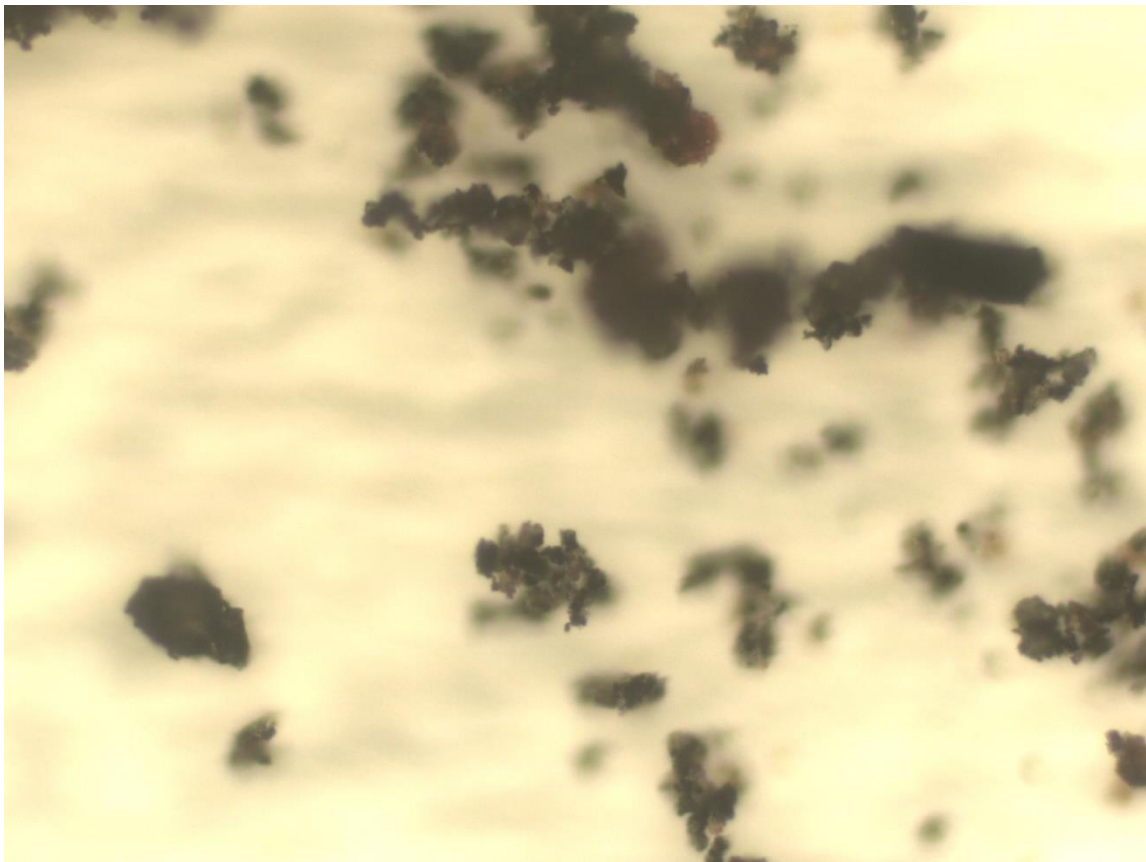


**Fig. 16—Reacted iron sulfide at 20x magnification.**

Although the chemical composition of the precipitation from Test 3 was unable to be identified, visual analysis suggests that the iron control agent was no longer in solution. The excess chemical that did not chelate iron ions precipitated onto the solid iron sulfide particles.

It was concluded from Test 3 that using a 1:1 molar ratio of iron to chelant was unsuccessful for iron sulfide dissolution tests due to only partial dissolution of solids.



## CHAPTER VI

### EFFECT OF HYDROGEN SULFIDE SCAVENGERS ON IRON SULFIDE DISSOLUTION

To determine the most efficient hydrogen sulfide scavenger, a series of tests were conducted, as shown in **Table 3**. All scavengers were tested at the same conditions of 320°F and 300-400 psi. The remainder of the acid system was 35 wt% Acid B, which was the organic acid, and 12 GPT of corrosion inhibitor. The corrosion inhibitor was used to protect the equipment and was optimized in later experiments.

Scavenger A was a high pH scavenger tested as 22 GPT and dissolved 54% of the iron sulfide during the reaction. It was hypothesized that the pH of greater than 9 scavenger was consuming the acid. The organic acid was lowering the pH of the system, therefore, less acid was available to react with the iron sulfide. Scavenger A was not further tested.

Scavenger B and Scavenger C were successfully used at neutral pH and surface conditions for scavenging hydrogen sulfide. However, both scavengers had not been tested in acidic conditions. Additionally, the scavengers did not perform well under high pressure and temperature. Scavenger B and Scavenger C were not further tested.

Scavenger D showed promising dissolution rates and a series of tests were conducted to determine the concentration to use in later experiments. As seen in **Fig. 17**, the scavenger concentration peaked between 25-30 GPT concentrations. Although 25 GPT had 1 wt% higher dissolution, 30 GPT was the concentration used for the rest of the acid development to decrease hydrogen sulfide evolution. At a concentration of 40 GPT, the

weight of the after reaction solids approximately doubled the initial weight. The scavenger precipitated and it was determined that 40 GPT was no longer in range of the system.

Test	Scavenger	Concentration, GPT	Dissolution, wt%	Remainer of System
1	A	22	54	35 wt% Acid B + 12 GPT CI
2	B	22	17.5	35 wt% Acid B + 12 GPT CI
3	C	21	11.5	35 wt% Acid B + 12 GPT CI
4	D	19	65	35 wt% Acid B + 12 GPT CI
5	D	25	79	35 wt% Acid B + 12 GPT CI
6	D	30	78	35 wt% Acid B + 12 GPT CI
7	D	35	75	35 wt% Acid B + 12 GPT CI
8	D	40	0	35 wt% Acid B + 12 GPT CI

**Table 3—Hydrogen sulfide scavenger experiments.**

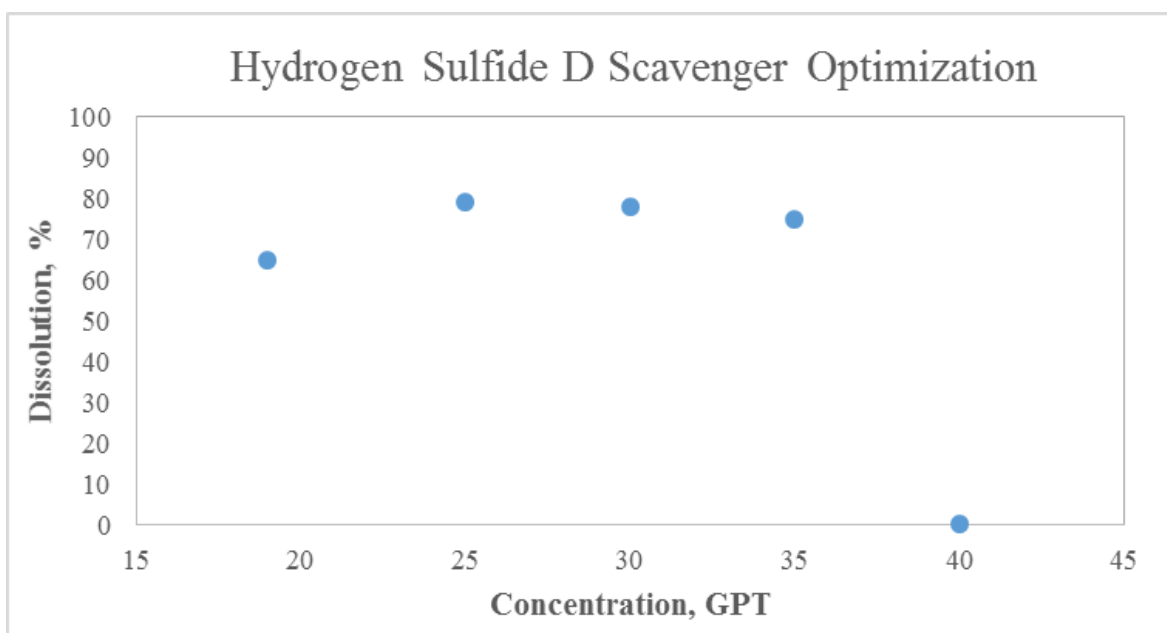


**Fig. 17—Hydrogen sulfide Scavenger D optimization.**

XRD analysis was used to analyze the 40 GPT test of Scavenger D. The results are shown in **Fig. 18** and **Fig. 19**. The precipitation noted in the weight gain of the sample was determined to be elemental sulfur and sjogrenite. Sjogrenite is a mineral that consists of hydrated magnesium iron carbonate hydroxide. Based on the precipitation and XRD results from the 40 GPT test of Scavenger D, it was determined that the system was overloaded and any higher concentrations would not be compatible with the system.

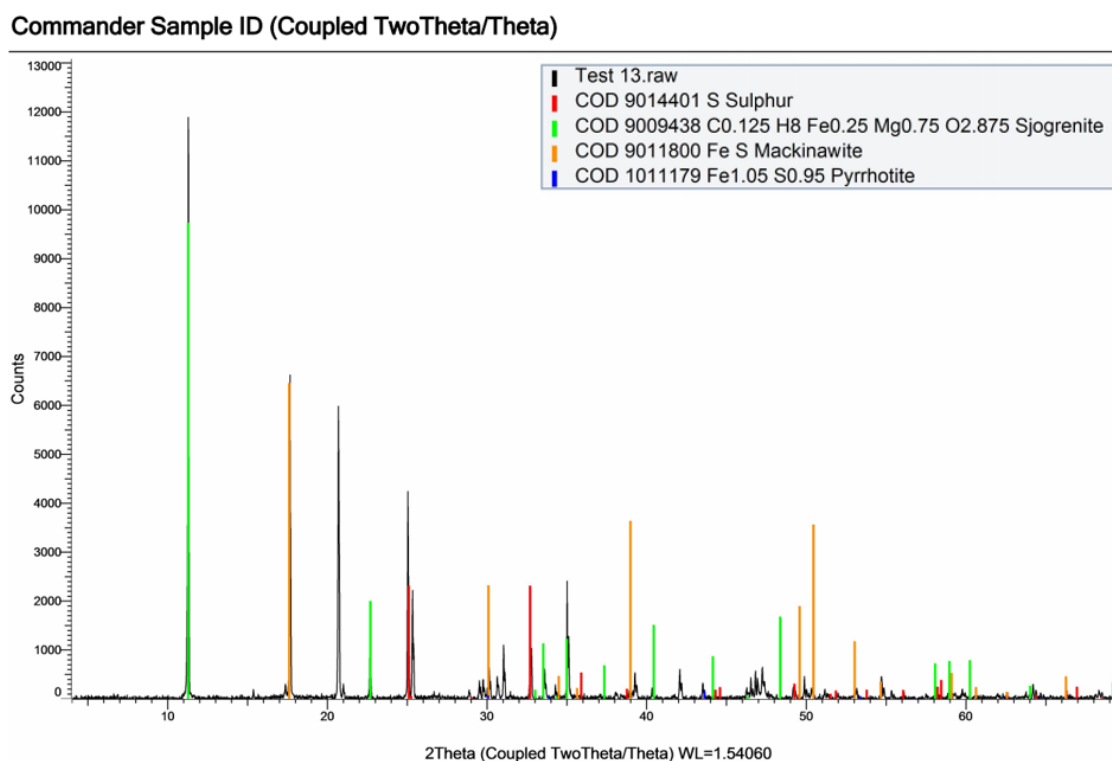


**Fig. 18—XRD analysis for 40 GPT Scavenger D experiment.**

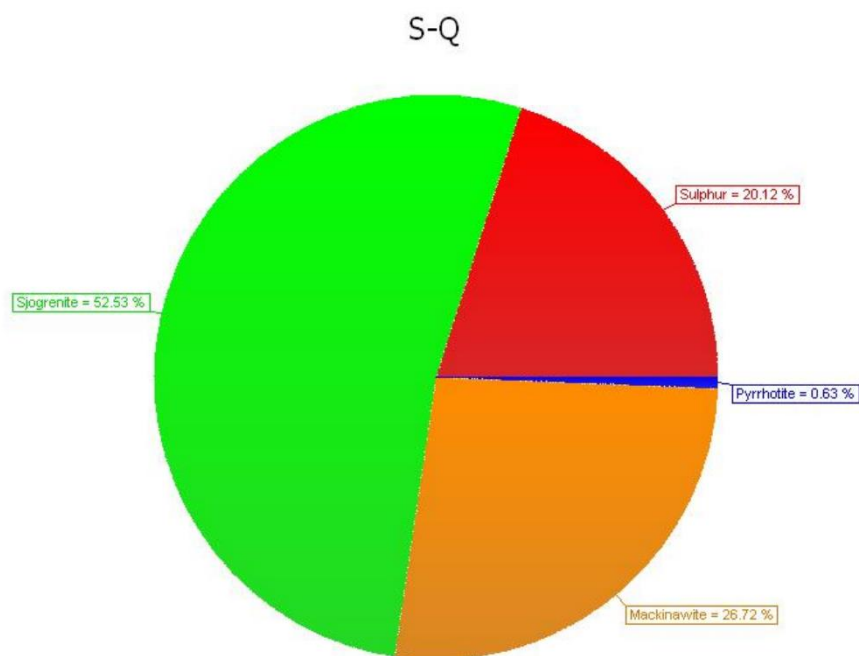


**Fig. 19—XRD analysis for 40 GPT Scavenger D experiment.**

## CHAPTER VII

### DESIGN OF EXPERIMENTS TO DISSOLVE IRON SULFIDE

Design of experiments was used to test three additives: a scavenger aid, an iron control agent, and a dispersant. Minimum and maximum concentrations were defined for each of the additives. The design of experiments is shown in **Table 1**. The objective of the initial eight experiments was to screen the different additives. This would allow for an understanding what additives would affect the system.

Pattern	Phase	Test #	Input			Output	
			Scavenger Aid	Iron Control	Dispersant	FeS Dissolution	H <sub>2</sub> S
			GPT	GPT	GPT	%	ppm
+—	I	1	6	0.5	1	51	120
—+	I	2	0.5	0.5	5	54	400
—+	I	3	0.5	20	1	72	380
+++	I	4	6	20	5	31	180
+++	II	5	6	0.5	5	45	300
—	II	6	0.5	0.5	1	42	170
—++	II	7	0.5	20	5	53	450
++—	II	8	6	20	1	44	220

**Table 4—Design of experiments concentrations and results.**

The scavenger aid had a minimum concentration of 0.5 GPT and a maximum concentration of 6 GPT. The iron control agent had a minimum concentration of 0.5 GPT and a maximum concentration of 20 GPT. The dispersant had a minimum concentration of 1 GPT and a maximum concentration of 5 GPT.

All design of experiment tests were conducted at the same conditions of 320°F and 1,300-1,400 psi. The base acid concentration used was as follows:

**Base Acid Concentration: 5 wt% Acid A + 15 wt% Acid B + 30 GPT Scavenger D +  
50 GPT CI + 50 PPTG Intensifier.**

The patterns of the design of experiments were designed to test minimums and maximums of each additive, defining the outer corners of a cube, shown in **Fig. 20**.

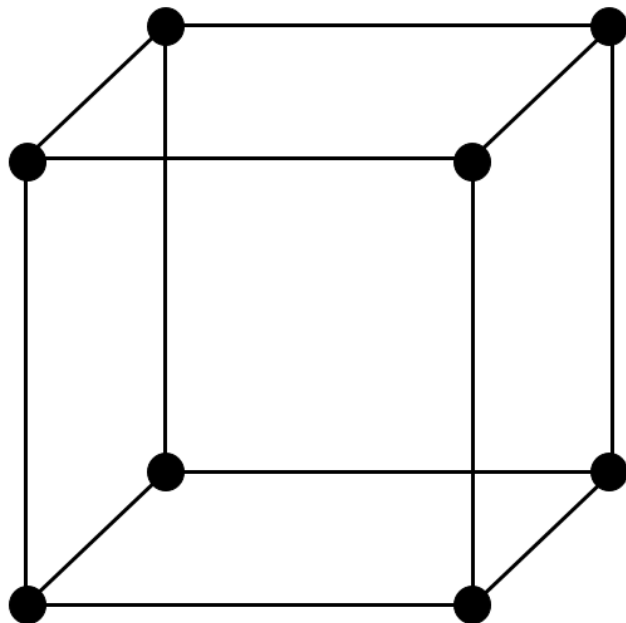


**Fig. 20—Design of experiments cube.**

After Phase I, it was determined that Test 3 had the best results with a scavenger aid concentration of 0.5 GPT, iron control concentration of 20 GPT, and a dispersant concentration of 1 GPT. The Phase I ranges of iron sulfide dissolution were between 31-72%. The hydrogen sulfide concentrations for Phase I were between 120-180 ppm. The lowest dissolution rate was seen when all three additives were maximized. The Test 3 results minimized the scavenger aid and dispersant concentrations, while maximizing the

iron control concentration. The best results from Phase I resulted in 72% iron sulfide dissolution and 380 ppm of hydrogen sulfide.

After Phase II, it was determined that Test 7 had the best results with a scavenger aid concentration of 0.5 GPT, iron control concentration of 20 GPT, and a dispersant concentration of 5 GPT. The Phase II ranges of iron sulfide dissolution were between 42-53%. The hydrogen sulfide concentrations for Phase I were between 170-450 ppm. The lowest dissolution rate was seen when all three additives were minimized. The Test 7 results minimized the scavenger aid concentration, while maximizing the iron control and dispersant concentrations. The best results from Phase I resulted in 53% iron sulfide dissolution and 450 ppm of hydrogen sulfide scavenger.

When analyzing both phase results of the design of experiments, Test 3 had the overall highest dissolution with an acceptable hydrogen sulfide concentration with a 72% iron sulfide dissolution rate and 380 ppm of hydrogen sulfide.

## CHAPTER VIII

### EFFECT OF PRESSURE ON IRON SULFIDE

Iron sulfide dissolution experiments were conducted to determine the effect of pressure on the dissolution rate. The acid formulation was the same for each experiment, and it consisted of 35 wt% Acid B + 30 GPT Scavenger D + 12 GPT CI. The testing temperature was 300°F. Reaction time between the acid and the iron sulfide solids was four hours.

For the first experiment, a pressure range of 400-500 psi was applied to the system. The dissolution rate of the iron sulfide solids was 78 wt%. In **Fig. 21**, the raw, overlaid with interpreted, results for the test at a lower pressure can be seen. Pyrite was noted, which is an iron sulfide mineral with a 1:2 molar ratio between iron and sulfur. This type of iron sulfide is unable to be dissolved by acids. Pyrrhotite was also interpreted in this sample, which has a 1:1 molar ratio between iron and sulfur. Additionally, quartz was interpreted in this sample. It is suspected that the quartz is due to contamination from the mortar and pestle. Lastly, a source of hydrocarbon was noted. This is due to the organic material in the acid formulation coating the solid particles. Although the after-reaction solids were rinsed with acetone and deionized water, there was still residue on the solid particles.

It should also be noted that a large peak at approximately 18 2Theta was unable to be identified.



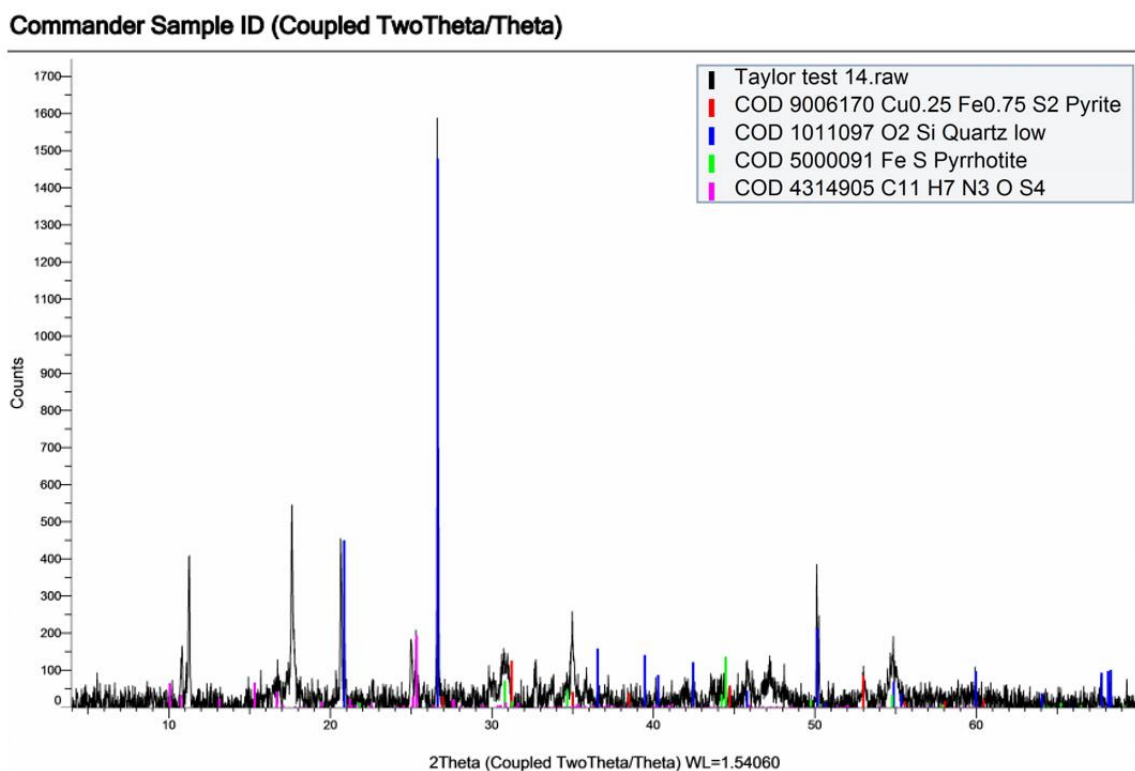


**Fig. 21—Interpreted XRD results for experiment using 400-500 psi.**

The quantitative results of the 400-500 psi experiment can be seen in **Fig. 22**. The after reaction solid sample consisted of 61% quartz, 26% of an organic substance, 7% pyrrhotite, and 6% pyrite.

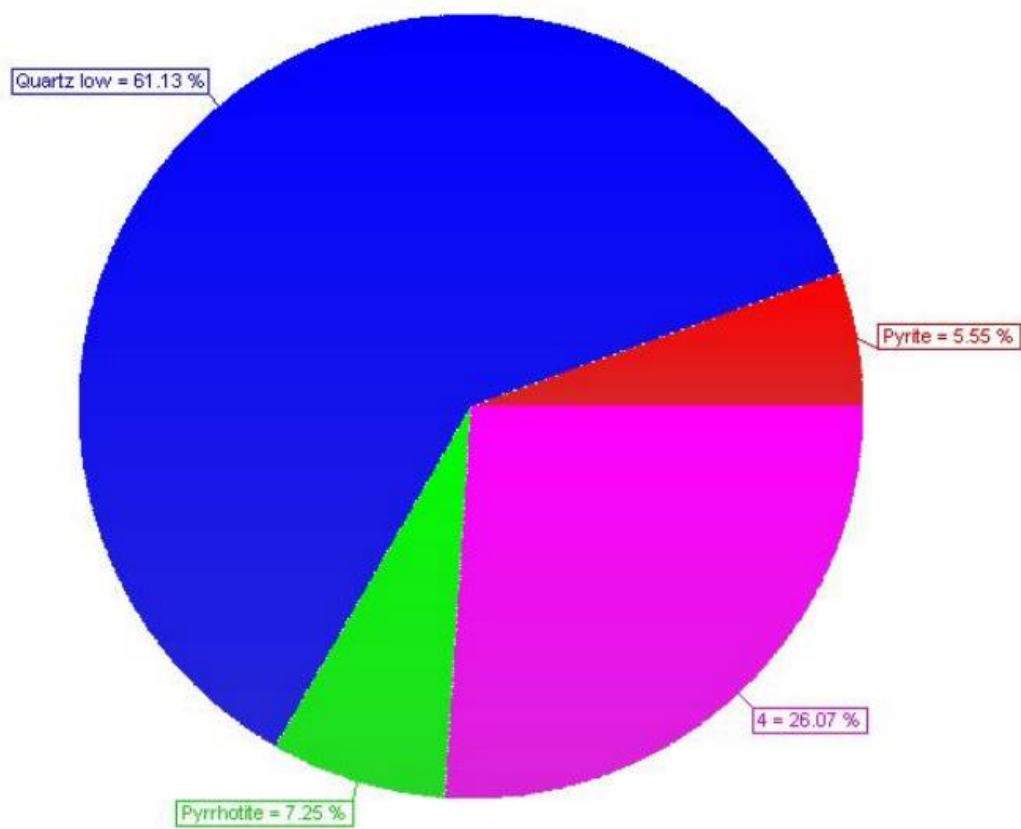


**Fig. 22—Quantitative XRD results for experiment using 400-500 psi.**

The **Fig. 23** shows the raw, overlaid with interpreted, results for the test using 1,300-1,400 psi. The dissolution rate for the experiment using higher pressure decreased to 55 wt% of the iron sulfide solid particles. It should be noted that the sample was noisy and interpretation was difficult. Picotpaullite, a common mineral found when mining sulfide ores, consists of tellurium, iron, and sulfur. Yavapaiite is a potassium, iron, and sulfate based mineral, which accounted for the majority of the interpretation. Pyrrhotite, a form of iron sulfide with the iron to sulfur ratio of approximately 1:1, consisted of 18% of the sample. The last element that was interpreted was quartz, an unexpected mineral. It is assumed that this is due to contamination of the sample during grinding with the agate mortar and pestle.

It should also be noted that a large peak at approximately 18 2Theta was unable to be identified.

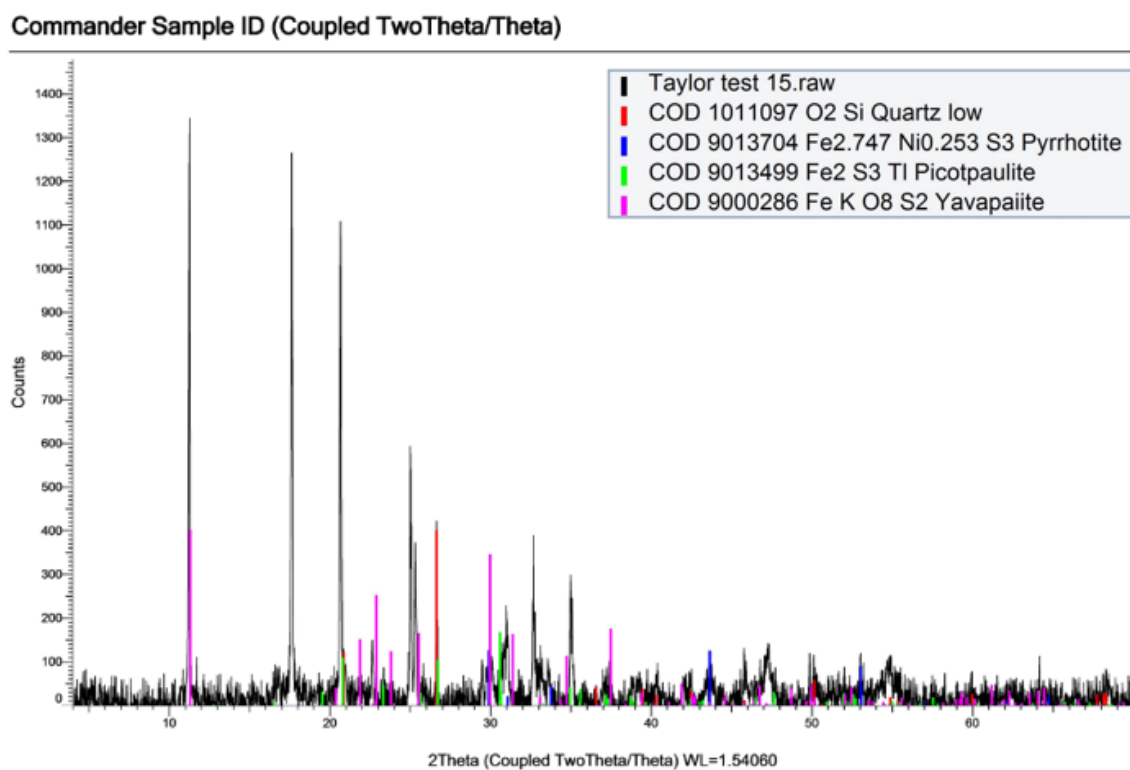


**Fig. 23—Interpreted XRD results for experiment using 1,300-1,400 psi.**

The quantitative results of the 1,300-1,400 psi experiment can be seen in **Fig. 24**. The after reaction solid sample consisted of 52% yavapaiite, 18% pyrrhotite, 23% quartz, and 7% picotpaulite.

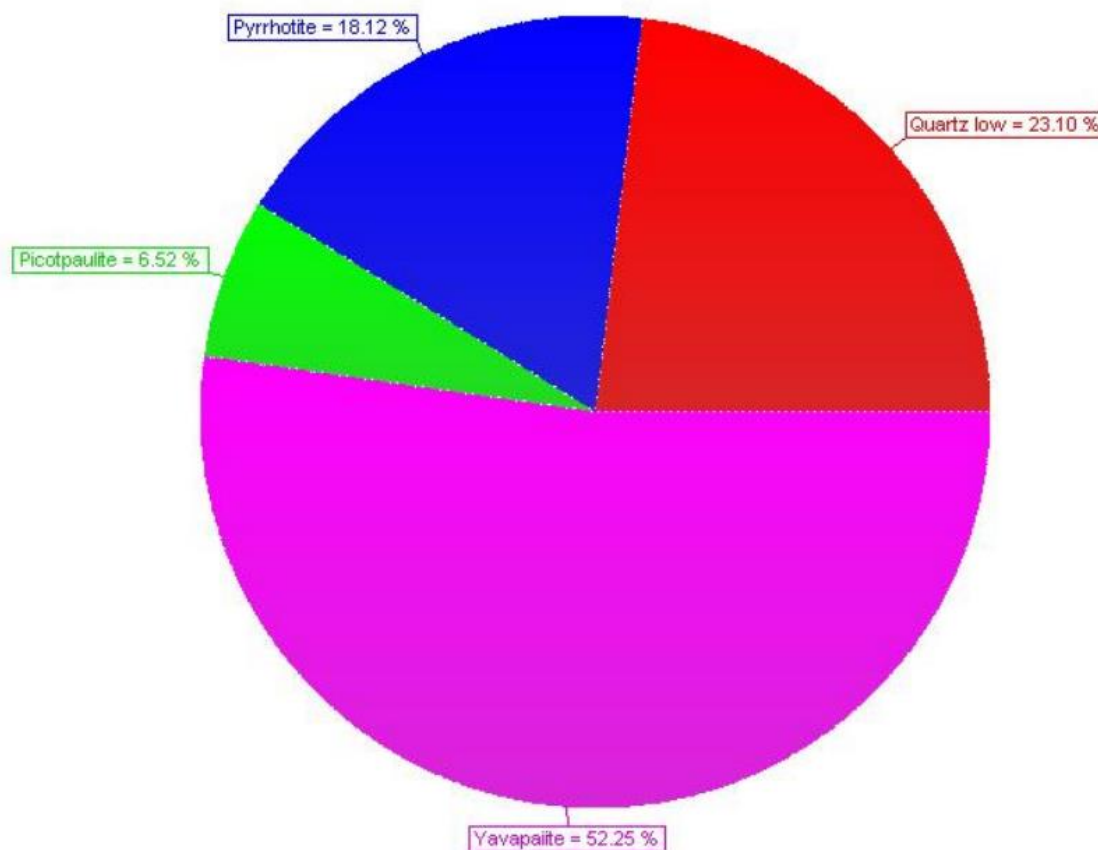


**Fig. 24—Quantitative XRD results for experiment using 1,300-1,400 psi.**

While increasing the pressure from 400-500 psi to 1,300-1,400 psi, the dissolution of the iron sulfide decreased significantly. At the lower pressure range, 78 wt% of the iron sulfide was dissolved, while at the higher pressure range, only 55 wt% of the iron sulfide was dissolved. Both tests were conducted at identical conditions.

Although the pressure increase did not change the mineralogical composition significantly, the decrease in dissolution was a negative effect. This is due to the reaction kinetics of the iron sulfide and acid reaction. Lawson et al. (1980) investigated the reaction rate of iron sulfide with hydrogen and identified the forward and reverse reactions (**Eq. 7**).

$$\text{Rate} = k_f[\text{H}^+] - k_r[\text{Fe}^{2+}]^{0.5}(\text{P}_{\text{H}_2\text{S}})^{0.5} \quad (7)$$

Where  $k_f$  is the forward reaction, controlled by the hydrogen atoms, and  $k_r$  is the reverse action, controlled by ferrous iron and the partial pressure of hydrogen sulfide. This reaction is important to note because as hydrogen sulfide stays in solution, the reaction does not progress. The dissolution treatment of iron sulfide needs to include a hydrogen sulfide scavenger to remove hydrogen sulfide in the reaction, which will maintain the forward reaction. A hydrogen source is needed to act as a dissolver for iron sulfide. This also supports that as pressure increases, the solubility of iron sulfide decreases.

In the higher pressure experiment, there was less available space for the hydrogen sulfide to move into the gaseous phase. These experiments show the importance of testing

the iron sulfide dissolver at the field conditions. A high pressure range of 1,300-1,400 psi was chosen due to limitations of the experimental set-up.

## CHAPTER VIII

### CONCLUSIONS AND RECOMMENDATIONS

#### 8.1 Conclusions

- The addition of the mineral acid changed the after reaction solid composition to 100% iron sulfide, according to XRD analysis.
- Iron sulfide solubility decreases with increased pressure.
- Adding iron control to the organic and mineral acid blend chelates the iron, which then decreases the iron to sulfur ratio.
- The base acid formula developed is 5 wt% Acid A + 15 wt% Acid B + 30 GPT Scavenger D + 50 GPT CI + 50 CI Intensifier.
- Following Phase 2 of design of experiments, it is recommended to investigate additional iron control additives for high temperature applications, as well as to investigate ways to reduce the amount of hydrogen sulfide gas released during the dissolution reaction.

#### 8.2 Recommendations

Several recommendations are made based on shortcomings in this research. These recommendations are regarding hydrogen sulfide measurements and release, pressure limitations, and corrosion inhibitor mixing.



Hydrogen sulfide is highly toxic in nature. A minimum of two scrubbing solutions are needed to neutralize the gases released from the iron sulfide dissolution tests. It is recommended that the scrubbers be conical to provide maximum contact time with the solution. When performing these tests, the set-up should be in a vacuumed room with a large fume hood.

The hydrogen sulfide should be tested at ambient conditions when using the Dräger tubes and hand pump. A new hydrogen sulfide compatible gas collection bag should be used for each experiment. When sampling the hydrogen sulfide, the pressure and temperature of the reaction should be approximately the same for every experiment.

Additionally, a correlation needs to be developed for hydrogen sulfide released in laboratory conditions to when it is released in field conditions from iron sulfide dissolution. It is industry standard that not more than 10 ppm should be around the well; however, because hydrogen sulfide is a measured concentration, it is not comparable to a one liter reactor. This correlation should be made for each well that will be treated.

Due to pressure limitations, these tests were not conducted about 1,400 psi. However, it was noted that pressure affects the dissolution rate. Additionally, increased pressure will affect the hydrogen sulfide concentration. Therefore, it is recommended that the final acid formulation should be tested at the approximate well pressure that the treatment will encounter.

The corrosion inhibitor used in this research was denser than the acid formulation. Therefore, settling was noted. It also agglomerated around the magnetic stirrer when mixing. By adding the corrosion inhibitor as the last chemical, it was able to be mixed by hand with a plastic syringe. The dispersion of the corrosion inhibitor was significantly higher when using this method, and it is recommended to do this for the remainder of the experiments.

## REFERENCES

- Bai, P., Zheng, S., Chen, C. et al. 2014. Investigation of the Iron–Sulfide Phase Transformation in Nanoscale. *Crystal Growth & Design* **14** (9): 4295-4302. DOI: 10.1021/cg500333p
- Bedford, C. T., et al, “The first Characterization of a Glyoxal-Hydrogen Sulfide Adduct” *J. Chem. Soc., Chem. Commun.*, 1035-1036, 1992.
- Buhaug, J., “Investigation of the Chemistry of Liquid H<sub>2</sub>S Scavengers”, Doctoral Thesis, Norwegian University of Science and Technology, 2002.
- Chakraborty, S., Lehrer, S., & Ramachandran, S. (2017, March 6). Effective Removal of Sour Gases Containing Mercaptans in Oilfield Applications. Society of Petroleum Engineers. doi:10.2118/183974-MS
- Cowan, J. K. (2005, January 1). Rapid Enumeration of Sulfate Reducing Bacteria. NACE International.
- Elkatatny, S. (2017, March 6). New Formulation for Iron Sulfide Scale Removal. Society of Petroleum Engineers. doi:10.2118/183914-MS
- Ford, W.G.F., Walker, M.L., Halterman, M.P., Parker, D.L., Brawley, D.G., and Fulton, R.G.: “Removing a Typical Iron Sulfide Scale: The Scientific Approach,” paper SPE 24327 presented at the 1992 SPE Rocky Mountain Regional Meeting held in Casper, WY, 18-21 May.
- Frenier, W.W., and Hill, D.G., 2002. Well Treatment Fluids Comprising Mixed Aldehydes. US Patent No. 6399547.

- Keenan, S., et al, "Inhibiting Corrosion Caused by Aqueous Aldehyde Solutions", US Patent No. 9068269 B2, 2015.
- Lawson, M.B., Martin, L.D. and Arnold, G.D.: "Chemical Cleaning of FeS Scales," Paper NACE 219, Corrosion/80, held in Houston, TX, March.
- Nasr-El-Din, H.A. and Al-Humaidan, A.Y. (2001) Iron Sulfide Scale: Formation, Removal, and Prevention. SPE 68315-MS. International Symposium on Oilfield Scale, 30-31 January 2001, Aberdeen, United Kingdom.
- Owens, T.R., Et al, "Triazine Chemistry: Removing H<sub>2</sub>S and Mercaptans". *ASRL Quarterly Bulletin* No. 155 Vol **XLVII** No. 3, October-December, pp. 1-21, 2010.
- Pohl, H.A. 1962. Solubility of Iron Sulfides. *Journal of Chemical & Engineering Data* **7** (2): 295-306. DOI: 10.1021/je60013a042
- Taylor, K.C., Nasr-El-Din, H.A. and Al-Alawi, M.: "Systematic Study of Iron Control Chemicals Used During Well Stimulation", SPEJ, 4 (1999) 19-24.

## APPENDIX A

### DETAILS OF EXPERIMENTAL METHODS

This appendix is to inform the user of the pre-startup requirements before utilizing the Parr 4523 reactor located in RICH 1010.

1. Required personal protective equipment (PPE):
  - a. Lab coat
  - b. Closed toed Shoes
  - c. Safety glasses
  - d. Long pants/jeans
  - e. Gloves (based on chemicals being used, refer to MSDS)
  - f. H<sub>2</sub>S monitor (if conducting experiments where H<sub>2</sub>S can be produced).
2. Verify fume hood is turned on
3. Verify all valves are in good working condition
4. Verify sufficient gas in N<sub>2</sub> tank for experiment
5. Check to make sure all lines are bled
6. Assemble scrubber (600 mL) (**Fig. 25**)
  - a. Determine fluid composition (may be NaOH to scrub sour gas or DI water if no CO<sub>2</sub> and H<sub>2</sub>S present)
  - b. Fill up scrubber to max of 90% of total volume, based on the estimation of gas needed to be neutralized with a safety factor (1.2-2)

- c. Ensure gasket in good working condition
  - d. Place two C clamps around top and bottom section (Gaps between clamps are acceptable)
  - e. Place metal ring around C clamps, aligning screw with hole in the C clamp and tighten screw.
  - f. Tighten six black screws on C clamp to ensure system is fastened
    - i. Use 9/16" wrench to tighten by hand (80%)
  - g. Lift assembled scrubber onto mounting platform ensuring that the viewing glass is facing outwards
  - h. Close metal latch and screw in securely
  - i. Attach reactor discharge line to scrubber
  - j. Establish vent line
7. Assemble reactor (1000 mL) (**Fig. 27** and **Fig. 28**)
- a. Load reactor with desired fluid filling to no more than 90%
  - b. Ensure gasket is in good working condition
  - c. Raise reactor vessel to head by pulling out spring loaded screw on the rail
  - d. Use 2 C clamps to connect the reactor vessel to the head
    - i. Use 7/16" wrench to tighten by hand (80%)
  - e. Lock clamps and tighten screws to ensure good fit
  - f. Attach heater (if needed)
    - i. Remove sensor probe
    - ii. Raise heater by pulling out spring loaded screw on the rail

- iii. Ensure reactor vessel is properly seated in heater
  - iv. Reattach sensor probe
8. Turn on controller to begin operation (**Fig. 28**)



**Fig. 25—Parr Reactor Scrubber (Assembled).**



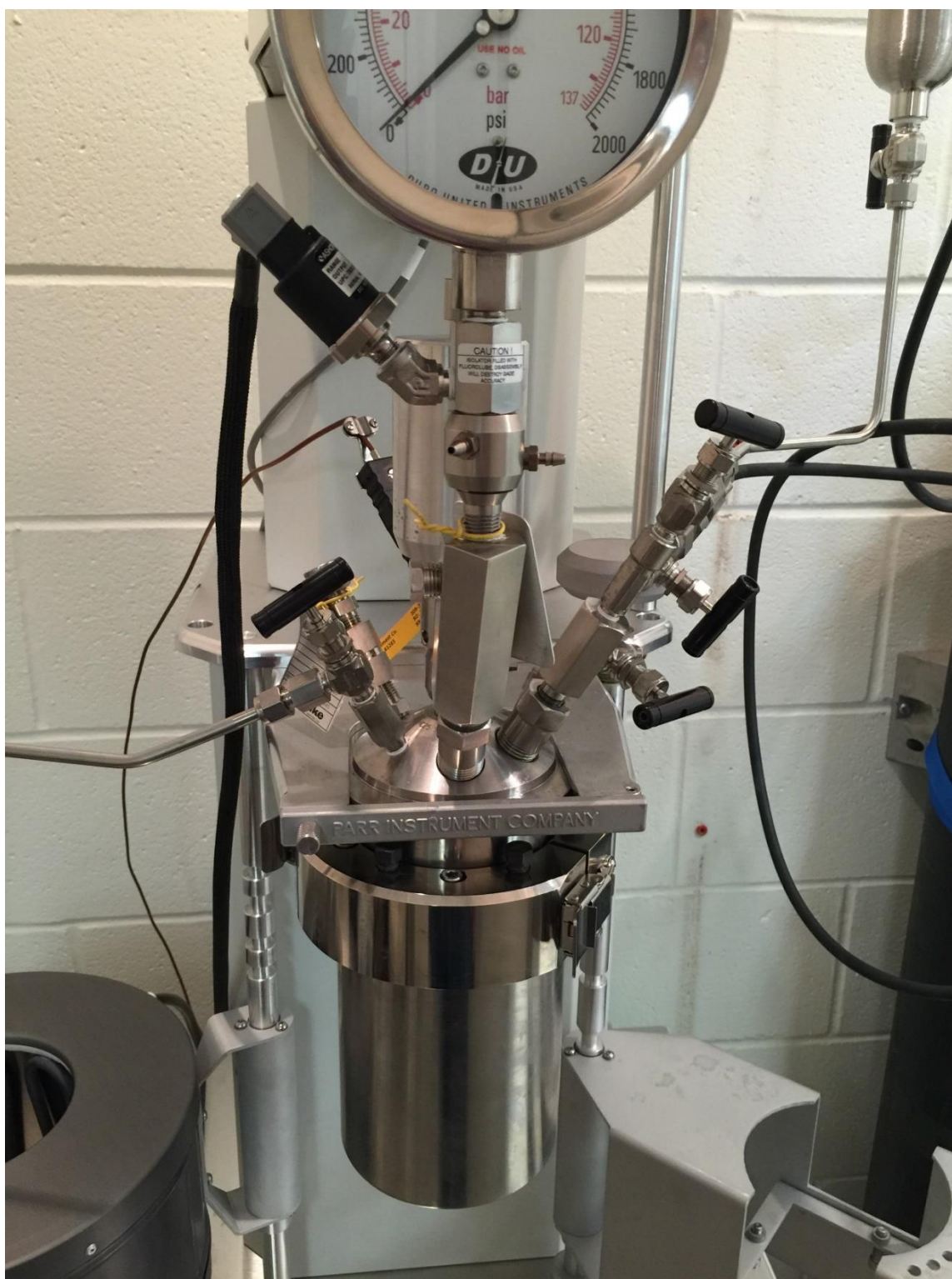


**Fig. 26—Parr reactor (assembled).**



**Fig. 27—Parr reactor (with heater attached).**





**Fig. 28—Complete assembled system.**

9. Pressurize inlet line
  - a. Open regulator to desired pressure. Use bleed valve to adjust (**Fig. 29**)
  - b. Open Line 1 to reactor to purge vessel and remove any excess oxygen (**Fig. 30** and **Fig. 31**)
  - c. Purge reactor for 1 minute
10. Pressurize system to desired pressure by adjusting reactor outlet valve
  - a. Desired pressure should be 200 to 300 psi less than required operational pressure (i.e. set to 700-800 psi if >1000 psi is required)
11. Bleed inlet lines of excess pressure
12. Connect heating element (if not already done before), and bring system to desired temperature by adjusting the set point of the Primary Temperature
  - a. ETLM Temperature refers to temperature of liquid
  - b. Primary Temperature refers to the temperature of the jacket
13. Conduct reaction for desired time (**Fig. 32**)

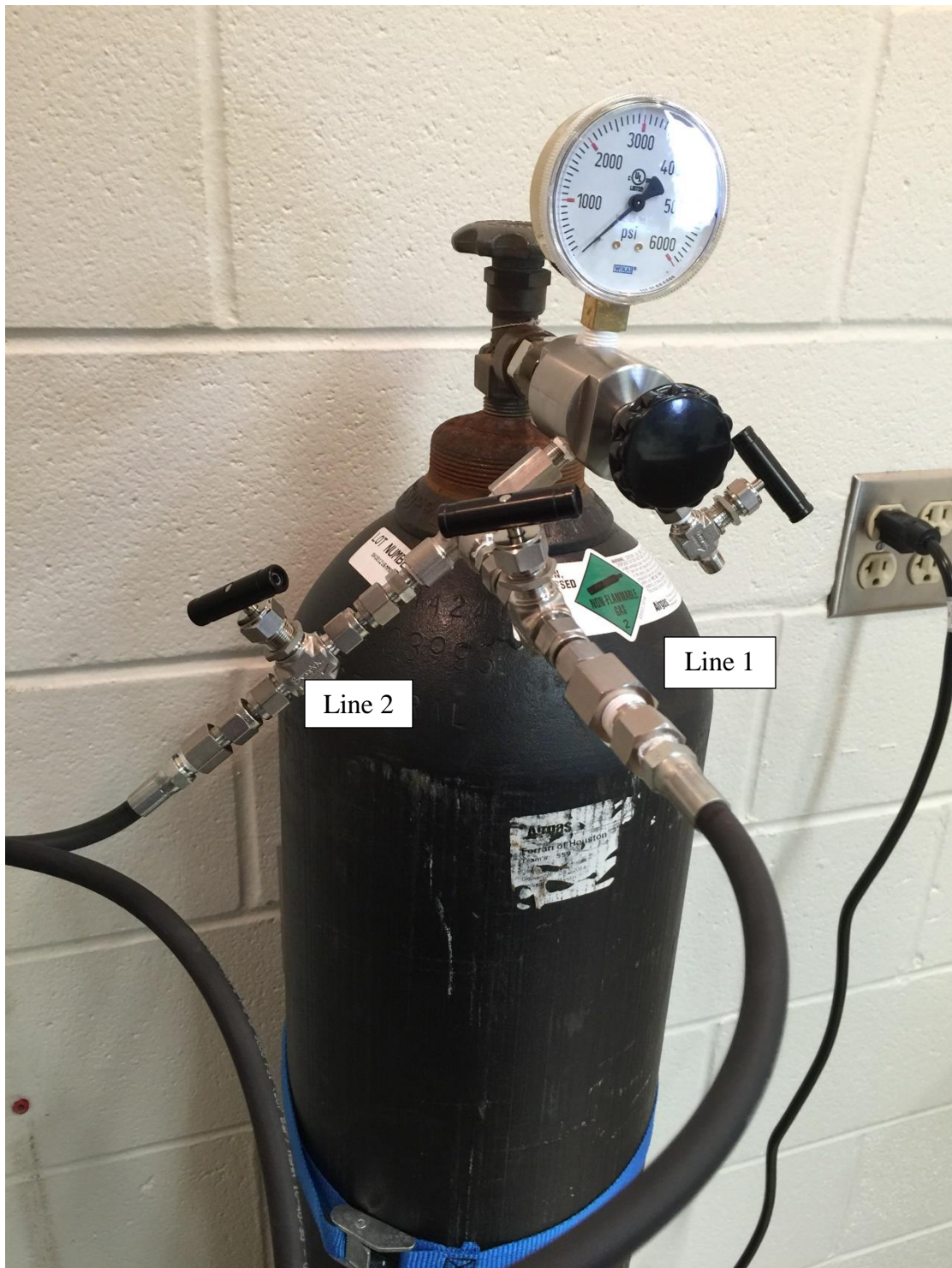


**Fig. 29—Inlet Configuration (1).**



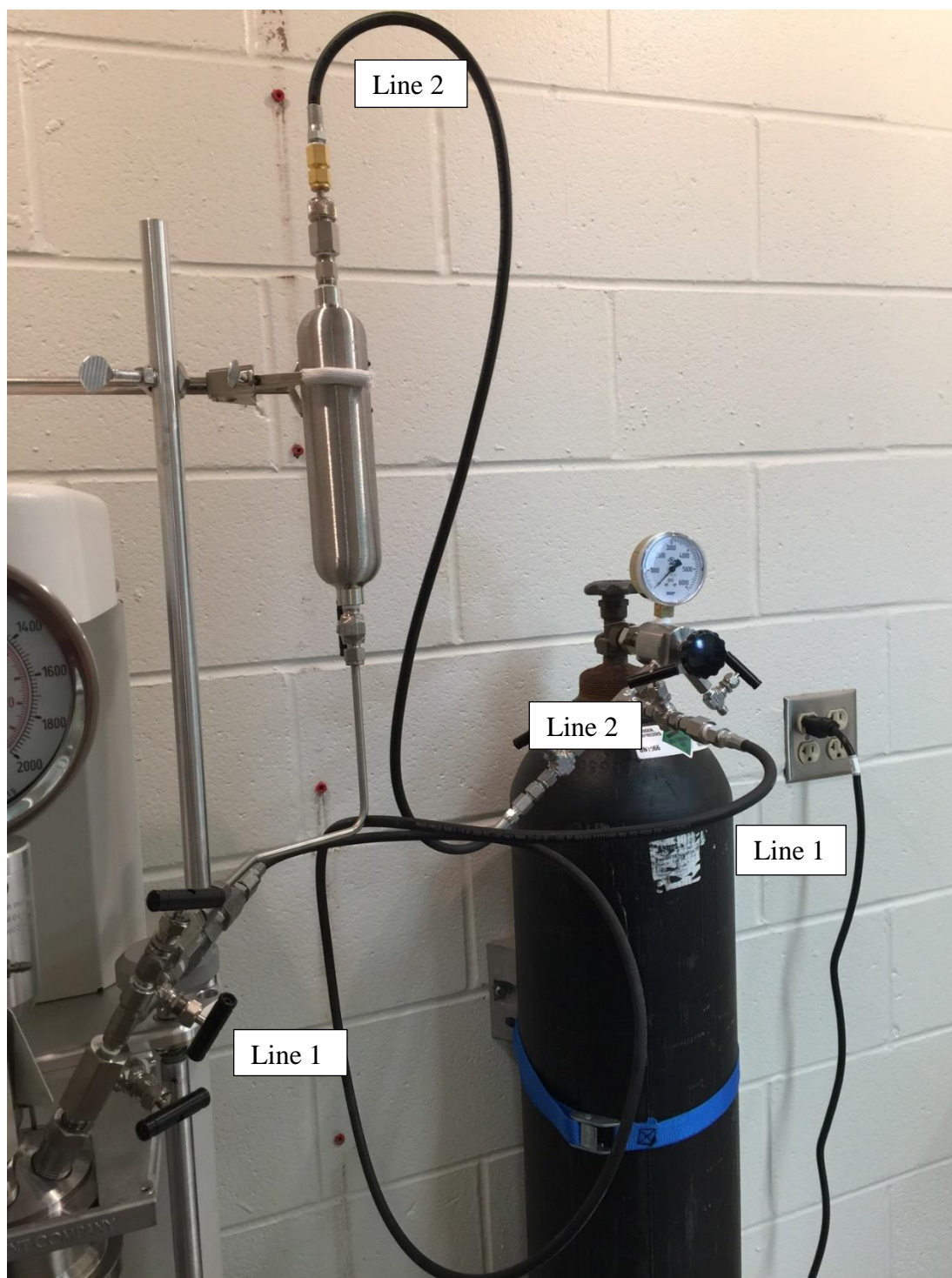


**Fig. 30—Inlet Configuration (2).**

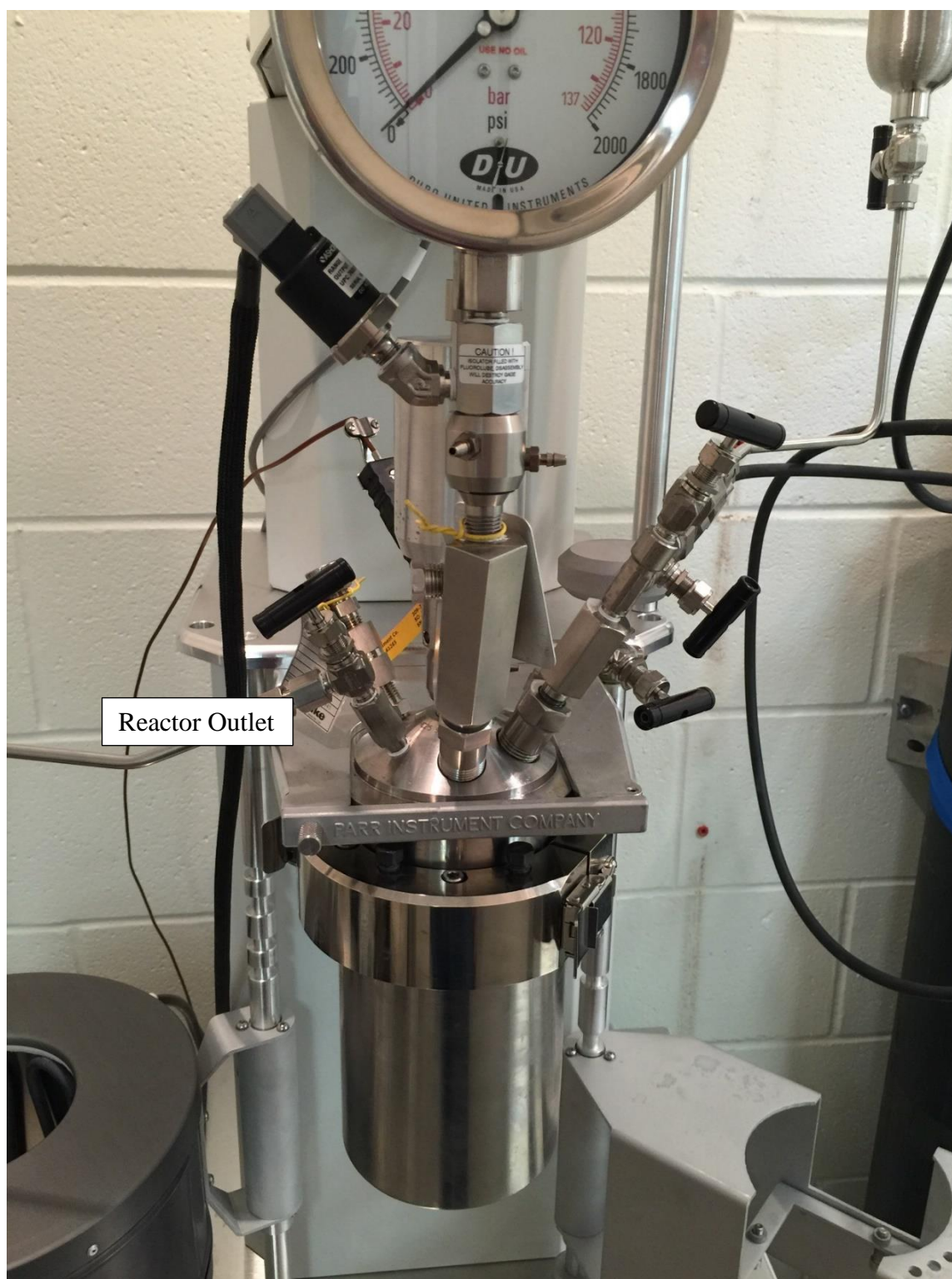


**Fig. 31—Inlet and outlets of reactor vessel.**



**Fig. 32—Parr 4523 reactor system.**